PROF. JAN ALEXANDER (Orcid ID : 0000-0002-2830-2727)

PROF. CHRISTOPHER FIELDING (Orcid ID : 0000-0002-2397-6116)

Article type : Original Manuscript

Controls on channel deposits of highly variable rivers: Comparing hydrology and event deposits in the Burdekin River, Australia

Running Title: **Burdekin River hydrology and event deposits**

Associate Editor – Charlie Bristow

JAN ALEXANDER[1*], CHRIS HERBERT[1], CHRISTOPHER R. FIELDING[2] and KATHRYN J. AMOS[3]

[1]School of Environmental Sciences, University of East Anglia, Norwich, NR4 7TJ, UK.

[2]Department of Geosciences, 214 Bessey Hall, University of Nebraska-Lincoln, NE 68588-0340, USA.

[3]Australian School of Petroleum and Energy Resources, University of Adelaide, SA 5005, Australia.

*Corresponding author j.alexander@uea.ac.uk.

ABSTRACT

Discharge event frequency, magnitude and duration all control river channel morphology and sedimentary architecture. Uncertainty persists as to whether alluvial deposits in the rock record are a time-averaged amalgam from all discharge events, or a biased record of larger events. This paper investigates the controls on channel deposit character and subsurface stratigraphic architecture in a river with seasonal discharge and very high inter-annual variability, the Burdekin River of north-east Australia. In such rivers, most sediment movement is restricted to a few days each year and at other times little sediment moves. However, the maximum discharge magnitude does not directly correlate with the amount of morphological change and some big events do not produce large deposits. The Burdekin channel deposits consist of five main depositional elements: (i) unit bars; (ii) vegetation-generated bars; (iii) gravel sheets and lags; (iv) antidune trains; and (v) sand sheets. The proportions of each depositional element preserved in the deposits depend on the history of successive large discharge events, their duration and the rate at which they wane. Events with similar peak magnitude but different rate of decline preserve different event deposits. The high intra-annual and inter-annual discharge variability and rapid rate of stage change make it likely that small to moderate-scale bed morphology will be in disequilibrium with flow conditions most of the time. Consequently, dune and unit bar size and cross-bed set thickness are not good indicators of event or channel size. Antidunes may be more useful as indicators of flow conditions at the time they formed. Rivers with very high coefficient of variance of maximum discharge, such as the Burdekin, form distinctive channel sediment bodies. However, the component parts are such that, if they are examined in isolation, they could lead to misleading interpretation of the nature of the depositional environment if conventional interpretations are used.

Key words: Antidunes, channel deposits, event deposits, high discharge variance river system, unit bars.

INTRODUCTION

Uncertainty persists as to the origins of alluvial deposits in the rock record, specifically whether they are predominantly a time-averaged amalgam of all flow events that a system experienced, or a more biased record of fewer, larger events (Sadler, 1983; Dott, 1983; Sambrook Smith *et al*., 2010). This uncertainty is particularly acute in evaluating the alluvium of streams which exhibit

extreme variations in discharge. The possibility that certain types of flow events may be disproportionately well-represented in the geological record is tacitly acknowledged in many publications (e.g. Ager, 1973; Bailey & Smith, 2010; Hajek & Straub, 2017; Paola *et al*., 2018) but has not been significantly quantified to date. This is because it has hitherto been challenging to create datasets that integrate hydrographic records, time-sensitive, serial imagery of riverbeds, and synchronized ground observations of those sites. This paper provides such a dataset and uses it to investigate the controls on surface deposit character and subsurface stratigraphic architecture in a river that produces very peaked hydrographs and has high inter-annual discharge variability, the Burdekin River of north-east Australia (Fig. 1A).

In March 2017, Tropical Cyclone (TC) Debbie caused heavy rainfall over part of northern Queensland Australia, including part of the Burdekin River catchment, and resulted in a discharge event that peaked at 11 955 $m^3 s^{-1}$ at the Clare gauging station (Fig. 2A: Data from the State of Queensland Department of Natural Resources, Mines and Energy). Research into the impact of this event on a reach of the lower Burdekin River (Fig. 1C) was undertaken initially with the rationale to consider whether large individual events such as that caused by TC Debbie would produce features in the deposit that could be diagnostic of such events in ancient deposits formed within comparable, highly-variable discharge systems. The observations in 2017, combined with previous observations at the same site (Amos *et al*., 2004; Fielding *et al*., 2005b; Herbert & Alexander, 2018; Herbert *et al*., 2019) led to analysis of the variation of rainfall-discharge responses in this catchment and the associated sedimentology. All of this research aims to refine the understanding of the sedimentology of variable-discharge rivers (cf. Fielding *et al*., 2009; 2011).

In the Burdekin River, most of the sediments are deposited during large-magnitude discharge events. Between the big events, a small volume of sediment moves in the low flow channel, there is a little aeolian and biological reworking and vegetation growth. Consequently, the architecture of the channel deposits results from a sequence of big events. This is unlike classic river architecture as illustrated by case studies from rivers with less variable discharge, epitomised by the Calamus River, Nebraska, USA (Bridge *et al*., 1998); the South Esk River, Scotland (Bridge *et al*., 1995); the South Saskatchewan, Canada (Sambrook Smith *et al*., 2010); and the Platte River, USA (Joeckel & Henebry, 2008; Horn *et al*., 2012).

Rainfall across the Burdekin catchment occurs mainly between January and April and is mostly short-duration, intense episodes associated with tropical cyclones and smaller-scale tropical depressions. Monsoonal troughs have variable contributions across the region in successive years. In the wet season, rainfall may be localized or widespread. Droughts may last several years and many end in sudden heavy rainfall events.

The Burdekin River has very highly variable discharge (Fig. 2); a characteristic of many rivers in the semi-arid, seasonal tropics. Most of the time (all of the dry season and through most of the majority of the wet seasons) the discharge is low or very low and most of the channel bed is sub-aerially exposed (Fig. 1C). Droughts may be of multiple year duration and cause prolonged low flow conditions. Intense rainfall causes very rapid stage rise and high magnitude discharge events. The river flow stays within channel in most years. The river channel scales with the peak flow of the major discharge events that may have return intervals *ca* 10 years (Alexander *et al*., 1999; Fielding *et al*., 1999). This is unlike most perennial systems in other climatic settings, where 'channel-forming discharge' events have return intervals of one to two years (Williams, 1978).

As is common for rivers in the seasonal tropics, the Burdekin River has a very high *coefficient of annual peak discharge variation* of 1.00 (cf. Fielding *et al.,* 2018). It is unlike other rivers in other parts of eastern Australia (Rustomji *et al*., 2009). Fielding *et al*. (2018) suggest that the sedimentary architecture of rivers with very high *coefficient of annual peak discharge* is distinct.

The average annual suspended sediment export of the Burdekin River to the Coral Sea has been estimated as 3.93×10^6 tonnes (80% confidence interval = 3.4 to 4.5×10^6 tonnes), based on 24 years of data (1986 to 2010; Kuhnert *et al*., 2012). However, the annual sediment export estimates ranged from 0.004 to 15.7×10^6 tonnes (Kuhnert *et al*., 2012), illustrating the wide variation between events. Bainbridge *et al.* (2014) found that discharge events with similar magnitudes could have substantially different suspended sediment loads. Higher suspended sediment loads have been recorded in drought-breaking floods (Mitchell & Furnas, 1996; McCulloch *et al*., 2003; Amos *et al*., 2004; Bainbridge *et al*., 2014). This is consistent with sediment availability being inversely dependent on vegetative ground cover (cf. Kuhnert *et al*., 2012).

The Burdekin Falls Dam (Fig. 1A) traps a lot of the sediment from the upper catchment and most of the coarse component of the load (all of the bedload from 88% of the catchment area)

(Lewis *et al*., 2013). Over a five-year monitoring period (2005/2006 to 2009/2010), Lewis *et al.* (2013) measured the trapping efficiency of the reservoir at between 50% and 85%. These authors found that particles <0.5 μm passed over the dam spillway; 50% of particles 0.5 to 5.0 μm were trapped in the reservoir; 75% of particles 5.0 to 30.0 μm were trapped and 95% of particles >30 μm were trapped. Most of the suspended sediment is transported through the river system to the sea and contributes only a very small proportion to the channel deposits, despite being up to 90% of the total sediment load of any discharge event. For example, in the 2000 discharge event that peaked at 11 155 m^3 s^{-1}, Amos *et al*. (2004) estimated that about 3.7 x 10^6 tonnes of suspended sediment and 3 x 10^5 tonnes of bedload were transported past the Inkerman Bridge on the coastal plain.

Fielding *et al*. (2011) observed that the distinctive characteristics of Burdekin River channel deposits and those of other lowland highly-variable discharge rivers: "*include: (1) erosionally based channel-fill lithosomes that exhibit complex lateral facies changes, with (2) abundant, pedogenically modified mud partings, (3) complex internal architecture that may lack the macroform elements typical of other fluvial sediment bodies, (4) an abundance of sedimentary structures formed under high flow stage (here termed Froude-transcritical and supercritical structures: FTSS), and (5) an abundance of in situ trees that colonize channel floors and are adapted to inundation by fast flowing water"*. Fielding *et al*. (2018) suggest that the channel deposits of highly variable discharge rivers are: "*characterized by an abundance of sedimentary structures indicative of Froude critical and supercritical flow, preservation of abundant remains of both in situ and arborescent vegetation and transported vegetational debris (and particularly large woody debris), pedogenically-modified mud partings within the channel deposit, abrupt lateral facies changes, and a paucity of macroform structure in the subsurface alluvial record*". These authors suggest that a wide range of bedding structures is preserved in a complex three-dimensional mosaic, and abundant woody material (both *in situ* and transported) and pedogenically modified mud layers within the channel body record multi-year droughts with low peak annual flow. Periods of multi-year droughts allow opportunistic tree species to grow on the channel bed, establishing groves that facilitate bar growth (Fielding *et al*., 1997).

The research presented herein supplies new data to refine the understanding of the sedimentology of variable-discharge rivers (cf. Fielding *et al*., 2009: 2011). In other settings, the temporal sequence of discharge events is known to create different geomorphic responses

including changes in channel and floodplain geometry (Harvey, 1984, Cenderelli & Wohl, 2003). The Burdekin River data confirm that similar rainfall events may produce flows with significantly different characteristics depending on antecedent conditions (cf. Alexander *et al*., 1999), and discharge events with similar peak magnitude may result in different event deposits depending on water and sediment routing, and the rate of change. This work establishes that the *flood duration* and *pattern of discharge fall* are also important controls on the nature of the deposits and features preserved on the bed.

This paper further suggests that the concept of dominant discharge (defined as that discharge which transports most bed sediment in a stream that is close to steady-state conditions; Carling, 1988) is of no use in highly-variable discharge systems because: (i) they are unlikely to reach equilibrium with their flows (never at steady-state); and (ii) the amount of work done by a flood depends not only on the peak discharge but also on the duration of exceedance of a critical discharge. This is also the case in arid settings (e.g. Graf, 1983; Tooth, 2000).

HYDROLOGY OF THE BURDEKIN RIVER

The large Burdekin catchment (*ca* 130 000 km^2; Fig. 3) varies from semiarid continental interior to wetter coastal terrain (Fig. 3A). The topography of the catchment is mostly subdued, locally rising to 1030 m in the Star River subcatchment within the Paluma Range in the north (Fig. 1A). The geology of the catchment is varied (Fig. 3B; Prosser *et al.*, 2002). The land use (Fig. 3C), topography and vegetation cover all affect the speed with which runoff gets into and down the river (e.g. Neil *et al*., 2002; Bainbridge *et al*., 2014).

The discharge in the Burdekin River and its tributaries is monitored at sites through the catchment (data from the State of Queensland Department of Natural Resources, Mines and Energy, available via bom.gov.au/climate). The river has been gauged at Clare continuously since 1949. This gauge is 52 km from the river mouth (Fig. 1B) and the drainage basin area above Clare is 129 876 km^2. A time-series of discharge recorded at Clare shows the magnitude of peak events and the variation within and between years (Fig. 2). The frequency distribution of discharge events suggests a natural 'break' or change in the distribution pattern between 7 500 m^3 s^{-1} and 10 000 m^3 s^{-1}, and another between 10 000 m^3 s^{-1} and 12 500 m^3 s^{-1}. In addition, anecdotal evidence (see Burdekin Shire's historic data www.burdekin.qld.gov.au/council/history-and-heritage/) suggests

that when discharge reaches about 14 000 m^3 s^{-1} water starts flowing from the Burdekin River into the Stokes Creek – Warren's Gully system (a system of linear topographic lows marking palaeochannels on the right bank, across the coastal lowland to the Coral Sea; Fig. 1B). Peak discharges of 10 000 m^3 s^{-1} and 14 000 m^3 s^{-1} at Clare are used herein to discriminate discharge event sizes at the study site. Over the last 50 years, there have been 23 discharge events with peak magnitude greater than 10 000 m^3 s^{-1} (Fig. 2, Table 1). The State of Queensland Department of Natural Resources, Mines and Energy define low flow level at Inkerman Bridge at 3 m, minor flood level as 7 m, moderate flood as 10 m and major flood depth as 12 m. All of the other events described in this paper as large peak-magnitude floods exceeded the moderate flood level at Inkerman Bridge.

At other reaches of the river system, similar discharge classes can be defined but as channel size differs, so does defining discharge. Individual runoff events may behave differently in different parts of the river. For example, attenuation of flood waves down the river system results in some events that are large magnitude in mid sections being only moderate peak events in the lower river. For example, in 1997, discharge measured at Sellheim peaked over 16 000 m^3 s^{-1}, but there was little rain in other parts of the catchment and the flood wave peaked at 7228 m^3 s^{-1} at Clare (Fig. 2B). Observations above Charters Towers at Big Bend and Dalrymple (Fielding *et al*., 1999; Fig.1A) suggest that this event reworked entire bars but it may have had little impact downstream at the study site near the Inkerman Bridge.

The Burdekin Falls Dam (Fig. 1A), 160 km upstream of the river mouth, impounds Lake Dalrymple (up to 1.85 km^3) and was completed in 1987. The mean annual peak discharges, measured at Clare before and since the dam was built, are 10 430 m^3 s^{-1} and 6813 m^3 s^{-1}. Since dam construction, early in the wet season, the discharge in the lower river is a little reduced as Lake Dalrymple fills, and the magnitudes of small to medium discharge events are reduced. The magnitude of large events (>10 000 m^3 s^{-1}: those considered in this paper) are little changed by the dam. The magnitude and steadiness of dry season flows appear slightly increased (about 7 to 30 m^3 s^{-1}) probably because of increased local irrigation runoff.

THE LOWER BURDEKIN RIVER STUDY REACH

The study reach (Fig. 1) is at the downstream end of a nearly straight, 10 km long section of the Burdekin River. The reach extends 10 km from Inkerman Bridge (19°38'8.58"S 147°24'14.40"E) to the diffluence of the main channel and Anabranch (first distributary; Fig. 1B). The channel bed is easily accessible and has been studied at intervals since 1998 (e.g. Amos *et al*., 2004; Fielding *et al*., 2005a, 2005b; Alexander & Fielding, 2006, Herbert & Alexander, 2018; Herbert *et al*., 2019). Fieldwork has included topographic surveying, observation of river and floodplain sediments, vegetation surveys, trenching, coring, sediment sampling (subsequent granulometry and compositional analysis), ground-penetrating radar surveys, observations and sampling of discharge events, and acquisition of rainfall and discharge data from other sources. Multiple aerial photographs (1994 to 1998) and satellite images (2006 to 2017) have been analysed. It has been possible to assess the changes in the bed morphology before and after some individual events.

The channel width within the study reach varies from 700 to 1900 m (mean 1187 m). The bank top height varies along each bank and bed-sediment mobilization during discharge events causes changes in channel depth in space and time. Consequently, there is little value in generalizing the bank-full depth over the study reach, but it is around 10 m (as at sections represented in Fig. 4). The main banks of the channel are generally steep and vegetated (including mature trees of various species). The channel floor is generally low gradient, sloping across or down the channel or composed of multiple ridges (Fig. 4). During the dry season, most of the riverbed is emergent and easy to observe, but the very deepest parts of the channel could not be observed directly or measured, because they are water-filled even in dry conditions. These lows can be seen in the photographs in Fig. 5 and represent a small proportion of the channel bed area. This pattern gives the low stage river the appearance of '*pool and riffle*', but the morphology is created by bar formation and bar movement during large discharge events. The pattern does not change much, if at all, at low stage (most of the year), but can change a lot over the short duration of individual large discharge events.

The prolonged exposure of large areas of riverbed allows riparian vegetation growth (ranging from grasses to trees), which subsequently influences sedimentary processes (Fielding *et al.*, 1997; Nakayama *et al.*, 2002; Herbert & Alexander, 2018). During wet periods, seeds germinate and plants continue to grow rapidly if their roots can reach the water table in the channel deposits. Through multi-year droughts, the riverbed vegetation can grow to considerable size (for example, Fig. 5). This sapling growth influences the subsequent bar development.

Saplings at the study site before the arrival of TC Debbie were up to about 4 m tall (Fig. 5A). Very large discharge events strip most, or all, of the vegetation from the channel bed, or bury it. Locally, there are some individual trees on topographic highs within the channel that have been estimated to be over 50 years old.

During most of the year, much of the channel sediment is dry and composed of moderately sorted coarse sand and gravelly sand that is compositionally immature, with pebbles and cobbles of a wide range of lithologies. Since completion of the Burdekin Falls Dam, coarse sediment moving in the study site is derived from: (i) reworking existing bed and bank sediment; (ii) input from the Bowen-Bogie catchments; and (iii) local runoff into the channel, whereas fine sediment comes from any part of the catchment. Sand from different parts of the catchment is not easily recognized, although that from the southern sub-catchments can be distinguished by the magnetic properties of magnetic inclusions within silicate grains (Maher *et al*., 2009). Since 1987 it is likely that little sand has moved past the Burdekin Falls Dam, but coarse sediment derived from the catchment above the dam before then is still moving down the lower river. Based on magnetic fingerprinting, sand fractions of suspended sediment samples from the 2000 Burdekin flood, collected from the Inkerman Bridge, appear to have had a different source compared with those from floods in 1998 and 1999 (Maher *et al*., 2009).

The sediment load ranges from clay-grade wash load to sand and gravel bedload (Amos *et al*., 2004). Mud accounts for a very small percentage of the channel bed deposits seen in trenches. In some years, mud drapes have been observed on the surface of the bed, most often restricted to local lower areas (Herbert & Alexander, 2018). They have been recorded also in some trenches (Herbert *et al*., 2020). The mud drapes are rarely more than 1 to 2 cm thick, and they desiccate, break into flakes and produce mud clasts. Mud also sometimes infiltrates the top of the sand and gravel bed (Herbert & Alexander, 2018). Sand is also carried in suspension in moderate and large events (Amos *et al*., 2004; Lewis *et al*., 2013), and a relatively high proportion of the floodplain deposits are sandy (Alexander & Fielding, 2006).

LARGE PEAK-MAGNITUDE DISCHARGE EVENTS AND RAINFALL PATTERNS

The runoff response to rainfall depends not only on the precipitation intensity, but also on the rain duration, aerial extent, soil infiltration capacity and antecedent conditions. Intense rainfall

associated with tropical cyclones and storms has been recorded within the Burdekin catchment exceeding 390 mm on 1 March 1988 at Home Hill (19.67° S 147.42° E) and 470 mm on 6 February 1947 at Kalamia Estate (19.52° S 147.42° E; Australian Bureau of Meteorology: www.bom.gov.au/climate/data/index.shtml). Rainfall recorded at Majors Creek (19.60° S 146.93° E), in an adjacent catchment, exceeded 510 mm on 11 January 1998 and 760 mm on 3 March 1946. Given the spatially erratic distribution of rain gauges over the area it is likely that intensities as high as or higher than these have occurred elsewhere within the catchment. Compared to tropical cyclones, a monsoon trough (as in 2000) produces more widespread but generally less intense rainfall, that may occur over a longer period (multiple days). Some of the variation in rain pattern is illustrated by the catchment maps of rain recorded in the seven days leading up to a big discharge event and those for the same duration after peak discharge (Fig. 6).

There is no widely agreed definition of *intense rain* as the use of the term depends on the experience of the individual, varying with climatic setting. Defining what an intense rainfall event is depends on the local conditions and on the timing resolution of rainfall data, and might be best related to local event frequency thresholds (cf. Groisman *et al*., 2005). In the more humid coastal areas of the Burdekin catchment, rainfall events with over 100 mm day^{-1} are called intense. However, inland in more generally arid areas of the catchment, 50 mm day^{-1} or less rain may have a big effect on soil erosion and river response, and can be called an intense rainfall event. The use herein of *intense rainfall* for these events is comparable with the use of 'intense rainfall' for short duration events of 20 mm per hour in the Caribbean (Barclay *et al*., 2007).

During or soon after a period of intense rain, the stream stage rises extremely rapidly (Fig. 7). The hydrographs measured at Clare, and other sites in the lower reaches of the Burdekin, record flood peaks moving down the system from different parts of the catchment such that the catchment network pattern, in addition to the rainfall intensity and distribution, influence the character of the discharge events at the study reach. The consequence of this is that similar rainfall volume/duration events may generate different discharge hydrographs depending on where in the catchment it rained, in addition to differences in rainfall events generating different patterns. Despite the large number of controls on the character and peak magnitude of discharge events, some size-duration patterns appear to be inherent in the system.

Based on magnitude and duration, the large peak-magnitude floods in the lower Burdekin River can be divided into three types:

1 Events that peak in 10 000 to 14 000 $m^3 s^{-1}$ range with short duration and rapid fall.

2 Events in the 10 000 to 14 000 m^3 s^{-1} range with gradual decline and a large total discharge volume.

3 The biggest events (>14 000 m^3 s^{-1}).

The distinction between Types 1 and 2 is seen in the rate of decline of the flood and the flood duration (Fig. 7A). The discharge in Type 1 decreases to half peak within 24 hours, whereas Type 2 declines to half peak in more than three days.

Events that peak in 10 000 to 14 000 m^3 s^{-1} range with short duration and rapid fall

In two of the events recorded at Clare that peaked in the range 10 000 to 14 000 m^3 s^{-1}, the water level receded very quickly, decreasing to half peak within 24 hours and below 2000 m^3 s^{-1} within 48 hours. These events occurred 2017 and 1988, when there was a short period of very intense rainfall on the eastern part of the catchment (Bowen-Bogie sub catchments; Fig 6). The same pattern of rapid rise and fall has also been observed in other parts of the Burdekin catchment in different years, notably recorded in mid reaches at Sellheim in 1997 (Fig. 2) when rain fell on the upper Burdekin catchment but not elsewhere. Discharge at Sellheim peaked at *ca* 17 800 m^3 s^{-1} and fell below 2000 m^3 s^{-1} within 48 hours.

The 2017 discharge event (Fig. 6) was the result of rain associated with TC Debbie. Tropical Cyclone Debbie made landfall as a Category 4 cyclone near Airlie Beach, Queensland on 28 March 2017 (Fig. 3D), and moved inland causing rain over the south-east part of the Burdekin catchment and other catchments to the south (Fig. 6). This was the first cyclone to hit Queensland in two years and followed five years of very low flow in the Burdekin River (Fig. 2). The sudden intense rain (for example, 36 mm hr^{-1} at 15:00 on 29 March at Urannah 20.92 S 148.32 E; Queensland Department of Natural Resources, Mines and Energy) caused very rapid runoff. Within the Burdekin catchment, rain fell mostly on the Bowen and Bogie subcatchments, which drain into the Burdekin River below the Burdekin Falls Dam. The western and northern parts of the Burdekin catchment contributed little to the flood event. At Inkerman Bridge, water level increased 6 m in six hours on 29 March 2017.

The intense rain and runoff caused land degradation, entrained large volumes of sediment, changed riverbed morphology and discharged a plume of freshwater and suspended sediment into the Coral Sea (Xiao *et al*., 2019). The sediment flux appears to have been particularly high (*ca* 1.5

million tonnes over six days: Lewis *et al., 2019*). This is probably because the intense rainfall followed a prolonged dry period. This is likely similar to the pattern recorded in other drought-breaking rainfall events (Mitchell & Furnas, 1996; McCulloch *et al*., 2003; Amos *et al*., 2004; Bainbridge *et al*., 2014).

Events in 10 000 to 14 000 $m^3 s^{-1}$ range with gradual decline

In the last 50 years, there have been 12 large discharge events in which the peak was in the range 10 000 to 14 000 $m^3 s^{-1}$, and in 10 of these the water level receded over a week or more. In some cases, as illustrated by events in 2000, 1998 and 1983, rain fell on north and central parts of the catchment. In others, illustrated by December 2010 and 2007, rainfall was more widespread (Fig. 6). In addition to those 10 large discrete events, there was another of similar character that occurred as a sub-peak of larger events in 1991. In this 1991 event, widespread rain caused discharge to rise gradually to a peak of 12 632 $m^3 s^{-1}$ on 15 January, after which discharge fell gradually.

The 2000 discharge event peaked at 11 155 $m^3 s^{-1}$ and the hydrograph recorded at Clare shows the very rapid rise and less steep falling limb (Fig. 7). In 2000, rain near the coast in January and February produced small flows in the river at the study site. Tropical Cyclone Steve took a track north of the catchment (Fig. 3D) and some associated rain fell on the northern parts. This was followed by rain associated with the monsoon trough along the coast and inland over the north of the catchment. The sediment transport behaviour in the lower Burdekin River in 2000 was supply-limited; peak bedload flux lagged peak discharge and the river could have transported more if more had been available (Amos *et al*., 2004). The water emanated from the catchment above the Burdekin Falls Dam and followed a moderately wet year.

The biggest events (peak over 14 000 $m^3 s^{-1}$)

In the last 50 years, 10 floods have peaked over 14 000 $m^3 s^{-1}$ at Clare. Three of these peaks occurred in 1991 (Fig. 7B), two in 2008 and two in 2009. Big events also occurred in 1978, 1989 and 2012 (Table 1; Fig. 2A).

For illustration, in 1991 the catchment was already wet at the start of the year and rain caused the discharge at Clare to rise rapidly to a peak of 15 709 $m^3 s^{-1}$ on 4 January (Fig. 7B), after which it fell rapidly before more widespread rain caused it to rise to 12 632 $m^3 s^{-1}$ on 15 January (Type 2 event). On 2 February 1991 rain fell over the Bowen-Broken River subcatchment, producing a discharge peak of 29 824 $m^3 s^{-1}$ at Clare on 3 February. This event had little contribution from the areas of catchment above the Burdekin Falls Dam, and the water level rose and fell very quickly. Discharge rose again to 12 269 $m^3 s^{-1}$ on 9 February, and again to 20 002 $m^3 s^{-1}$ on 21 February. Thus, not only were there three individual very big peak magnitude events, there were also two big events that would individually fit into other categories above. Discharge was high throughout the first three months of the year.

The consequence of this was widespread reworking of most bars in the channel (cf. Fielding *et al*., 1999). Thus, 1991 effectively 're-set' the channel architecture. In addition, the duration of high flow would have allowed large bedforms to grow and give more time for large-scale cross-stratification to form, consistent with the observations from ground-penetrating radar (GPR) data presented by Fielding *et al*., 1999, 2011).

The 2008/2009 wet season differed from that in 1991 in that most of the discharge in the river was from the upper Burdekin subcatchment. It was a double-peaked event reaching a maximum of 19 514 $m^3 s^{-1}$on 6 February 2009 and 15 845 $m^3 s^{-1}$ on 24 February. The discharge measured at Clare stayed above 9500 $m^3 s^{-1}$ for 15 days. Anecdotal evidence, and comparison of satellite images from the year before and after, suggest major changes in the pattern of the riverbed through this event.

SEDIMENT FEATURES AND RESULTING FACIES ASSOCIATIONS

The channel bed examined on emergent surfaces and trenches at the study reach is dominantly coarse to very coarse sand and gravel. Sediment sampling during discharge events (e.g. Amos *et al*., 2004; Bainbridge *et al*., 2012; 2016; 2018) indicates transport of vast quantities of clay, silt and fine sand, but little of this is deposited in the reach. Sand and gravel is transported on the bed and in near bed suspension in big events (Amos *et al*., 2004). This is observed on the bed and lodged in riparian trees above the bed (Fig. 8).

The channel bed is characterized by seven components: (A) sand sheets (dune fields, washed out dune fields and upper stage plane beds; (B) mud sheets; (C) gravel sheets; (D) antidune trains; (E) unit bars; (F) vegetation-obstacle marks or 'fields' of such obstacle marks; and (G) vegetation-generated bars, each of which form characteristic sedimentary packages. These can combine into complex bars, or channel aggradation packages.

A. Sand sheets

Extensive sand sheets occur both as stoss-side components of unit bars and adjacent to unit bars at all elevations in the channel. When observed on the emergent bed in dry seasons, their upper surface may be upper phase plane beds, dunes or washed out dunes (Fig. 8B). The sheets range in thickness from a few millimetres to tens of centimetres, and lateral extent from tens to hundreds of metres. The internal character ranges from planar lamination to cross-stratification. The sheet shapes vary, tending to be wedge shaped when formed on the stoss-side of unit bars and more lens shaped in other sites.

B. Mud drapes

Mud drapes are commonly observed on the emergent bed, sometimes restricted to local topographic lows, and are seen in locally in trenches (Fig. 8C). They vary in thickness from millimetres to several centimetres. Invariably they become desiccated soon after deposition. Where the drapes are millimetres thick and resting on coarse sand, desiccation can lead to mud curl formation (Fig. 8D) and these mud curls are easily reworked by small runoff events.

Mud sheets form during the waning phase of any size flood, so they are not indicative of low flow conditions. They occur at all levels in the channel and are preserved at all levels in the deposit, both as layers and as mud chips. Mud drapes tend to form when water level is relatively static or falls slowly over a few days following a bigger event. This appears more common in intermediate stages; mud drapes have been observed at low and intermediate heights on the emergent riverbed. Although occasionally they are extensive over areas tens to hundreds of metres long, they are generally discontinuous, occurring particularly in areas where flow is slowed such that silt may settle from suspension. On high areas of the riverbed this generally only occurs in areas where water is temporarily pooled (for example, in the troughs between unit bars, or in scour hollows near riverbed trees).

The amount of the mud in the channel deposits and in the floodplain deposits (Alexander & Fielding, 2006) is not indicative of the proportion of the sediment load that is mud (Lewis *et al*., 2013; Bainbridge *et al*., 2016) because most of this is washed through the river.

C. Gravel sheets and lags

Gravel moves over the bed as isolated clasts, rolling, saltating and sometimes in modified suspension (Amos *et al*., 2004). It moves both as isolated clasts and probably also as 'carpets' over the bed. Gravel sheets have lateral extents varying from a few metres to hundreds of metres (Fig. 8F). Their thickness is rarely more than one pebble or cobble thick but can be thicker in more laterally extensive sheets. Gravel streaks are locally observed on flat portions of the channel bed illustrating the path of pebbles and cobles over the surface. Gravel lags are observed in the lee of bars and obstacles and also in scours (for example, horseshoe shaped scours formed upstream of riverbed trees) where the gravel bed shape and extent are controlled by the scour. In places, gravel sheets were partially split into structures inferred to be of antidune origin. At some sites trains of antidunes were fully formed, suggesting that there is a spectrum observed from irregular gravel sheets to preserved antidune trains.

In the study reach the gravel is dominantly pebble or cobble grade. Where observed in trenches, the gravel sheets and lags generally have sand matrix, which may have been deposited with the gravel or infiltrated subsequently. The fabric (for example, visible in Fig. 8E) varies, but is generally imbricated either long-axis transverse or locally long-axis parallel to interpreted flow direction.

D. Antidune trains

Antidunes have been observed on the bed of the Burdekin River at several different sites and after discharge events of differing magnitudes. In 2017, antidunes were observed in two locations ('Inkerman' and 'Jarvisfield'; Fig. 1C). Antidunes were observed in trains of up to six, with near parallel crestlines transverse to high-flow direction. The plan-view crest shapes varied from near straight to linguoid. At the Inkerman locality, the mean wavelengths within antidune trains were between 16.4 m and 28.8 m and the amplitude measured on the emergent dry bed was 0.2 to 0.5 m. Further downstream at the Jarvis site, the wavelengths were as much as 30.7 m. All of these antidunes had steeper stoss than lee sides (3 to 14^{o} and 1 to 6^{o}, respectively). The antidunes were particularly recognizable where they had an elongate gravel patch along their crests (Fig. 9A).

Antidunes may have been overlooked where there was no gravel patch as their topographic expression is low. Within the Inkerman antidune field, the width of gravel patches at antidune crests varied up to one third of the mean antidune wavelength. When examined in section, the gravel deposits consist of a lens of sandy gravel (Fig. 9B). A trench through one of these contained downstream dipping cross-stratification.

The 2017 antidunes were very similar in morphology and grain size to antidunes described at mid-catchment Burdekin River sites by Alexander & Fielding (1997). These authors observed trains of between three and 12 parallel-crested bedforms with straight to slightly sinuous crests, wavelength from 8 to 19 m, and preserved amplitudes up to 1 m. In the antidunes described by Alexander & Fielding (1997) the gravel lenses contained single sets of low-angle downstream-dipping cross strata, picked out by gravel stringers. The grain fabric within the gravel was steeply dipping.

Trains of antidunes are recognizable on satellite images and aerial photographs and have been recorded on the ground in some years such as 2017, while in other years, such as in 1998 (reported by Fielding *et al*., 2005b) no antidunes were observed.

E. Unit bars and bar deposits

Relatively unmodified bars with morphologies that have developed mostly from depositional processes are termed unit bars (cf. Smith, 1974). In the Burdekin River, unit bars (Fig. 9C) are a common feature found across all but the highest elevations of the exposed riverbed (Herbert *et al.,* 2019). They may form and move in individual discharge events and may persist for several small to moderate sized events.

Unit bars examined in the 2015 to 2017 field campaigns were hundreds of metres long and wide, and up to 0.5 m high (Herbert *et al*., 2019). Their profile consisted of a very shallow dipping, planar stoss side that changed down-palaeoflow into a high-angle avalanche face. Some bars had superimposed dunes on their stoss, which were often preserved on the dry riverbed in partially washed out forms (presumably modified during falling stage). Well-preserved superimposed dunes were more common in 2017, and these were up to 0.1 m high and 0.9 m long. Dunes also commonly flanked the margins of unit bars in 2017.

Trenches through unit bars in 2017 (for example, Fig. 9D; see also Herbert *et al*., 2019) showed that the internal structure was dominated by co-sets of down-climbing cross-stratification (<0.4 m thick). Individual sets tended to thicken as they down-climbed. In most bars, there was a transition down-flow from down-climbing cross-stratified facies into a single, relatively thick (<0.5 m) but short (<1 m long), planar cross-stratified deposit close to their avalanche face. Overlying these deposits were topsets of thin (<50 mm), planar-stratified and low-angle cross-stratified sets with multiple internal truncation surfaces. Thin, localized bottomsets (<100 mm) of gravelly mud were observed infrequently (cf. Herbert & Alexander, 2018).

Ground penetrating radar data collected in 1999 (see fig. 6 in Fielding *et al*., 2011) show cross-stratification on the scale of 2 to 5 m sets in the lower part of the channel fill. In places there is evidence of smaller sets migrating over the bigger sets. The authors have no direct way to establish how these formed, but it is likely that they record advancing bar fronts. Fielding *et al*. (2005b) reported that: "*During the 1998, 1999, and 2000 dry seasons (May to October), large parts of the exposed riverbed surface were plane beds associated with isolated slipfaces or surfaces sloping gently towards the low-stage channel. Small parts of the surface, particularly near the low-stage channel, were gravel-armored. Elsewhere, bar surfaces were covered by fields of sinuous-crested dunes (amplitude up to 0.8 m), or locally larger, flat-topped, linguoid bedforms* [unit bars]". The preceding wet season included a flow of 11 905 $m^3 s^{-1}$ in January 1998, but 1992 to 1997 were dry years. Therefore, it is likely that these large bar sets formed in the very large discharges of 1991 (see below).

F. Vegetation obstacle marks – scours and sediment tails

Obstacle marks (Fig. 9E) result from deformation of flow by obstacles in a current (Dzulynski & Walton, 1965). Vegetation obstacle marks (cf. Nakayama *et al.,* 2002) consist of a scour around the plant(s) and a tail of sediment deposited in the lee-side separation eddy. The amounts, types and sizes of plants occurring in the channel at any one time are controlled by the interval since inundation, the species germination and growth rates, as illustrated by photographs before and after the 2017 discharge event (Fig. 5). Herbaceous vegetation germinates and grows rapidly but because of the aridity and coarse sediment of the channel floor, does not persist if there is a multiple-year drought. In contrast, some species germinate and grow rapidly and are either drought-resistant or have long roots. Most channel floor vegetation is removed, irrecoverably

damaged (by breakage, abrasion or immersion) or buried by the successive event, but some species are adapted to persist under successive immersion.

G. Vegetation-generated bars and channel bed in situ trees

Where areas of the bed are emergent for several years, dense groves of saplings become established. The principal types are species of *Melaleuca* and *Acacia*. In the lower river, as illustrated herein from the study site downstream of Inkerman Bridge, there are very few individual trees observed that were evidently more than about 10 years old, and most appeared less than five years old (judging from the relationship between trunk size and age presented by Fielding *et al*., 1997). This contrasts with the more common occurrence of older trees in the riverbed at a mid-catchment study site near Charters Towers (Fielding *et al.*, 1997). The reasons for this may be more frequent major inundation and also thicker channel bed deposits in the lower river; at the upper river site, tree roots may grow down below the basal erosion surface so that they are less likely to be uprooted. Fielding *et al*. (1997) and Fielding & Alexander (1996) demonstrated that saplings of the paperbark tree *Melaleuca argentea* that grow quickly in the channel influence sediment transport and bar formation (Fig 9F). The bars are elongate parallel to the tree groves, which may be aligned with or near to the channel direction. They are ridges of sand and gravel that extend through the grove and in a tail on its lee side. Internal structure of such bars includes common internal erosion surfaces with single clast gravel layers linings and sets of cross-bedding aligned in multiple directions.

In the lower Burdekin River, the five years prior to the TC Debbie flow of March 2017 were a period of low discharge (Fig. 2). During this time, aerial imagery shows that significant portions of lower bar surfaces became vegetated by opportunistic plant types. Among these, *Melaleuca argentea* was the most common, but two *Acacia* species also grew in sizeable groves, and other opportunists, including shrub-like woody weeds, were locally represented. Dendrochronological examination of tree cross-sections in July 2017 indicated that most of the saplings (all of those in lower areas of the channel) were less than five years old. Before the March event, the young trees appeared healthy and upright and closely-spaced. In July 2017 saplings had been substantially excised over large parts of the lower bar, and equally large areas were covered in dead trees, while in other areas the trees appeared substantially undamaged. Of the different

opportunistic vegetation types, *Melaleuca* was evidently best adapted to survival owing to its specialized strategies (Fielding *et al*., 1997) of flexible branches, elongate leaves, upstream-trailing roots in the subsurface, thick, spongy bark and subaerial root networks. After flooding, *Melaleuca* continue to grow well in inclined to prostrate stances. Other tree types, notably *Acacia longifolia* tended to be toppled by the flow. In July 2017, many dead *Acacia* were observed to have been toppled by rotation of the entire tree, and were partially or completely uprooted or exhumed from their substrate. Other upright trees and saplings had been snapped at heights of 1 to 2 m from the bed. The greatest variability in bar topography was found among groves of mostly dead *Acacia* trees, whereas linear groves of mostly live *Melaleuca* showed subdued topography.

DEPOSITIONAL MODELS FOR THE THREE DIFFERENT STYLES OF DISCHARGE EVENT

Although all the big events in this river system produce all the facies associations described above, the proportions of them differ as do their position and detailed characteristics among the three flow event types.

1. Events that peak in 10 000 to 14 000 $m^3 s^{-1}$ range with short duration and rapid fall

In comparison with fluvial deposits in other climatic settings, more high-stage features are preserved in all runoff events because of the rapid waning. However, in these events with rapid onset and very rapid falling stage, such features are even better preserved. After Type 1 events, the riverbed will preserve areas of gravelly antidunes, ‘washed-out’ dunes, dunes and plane bed with primary current lineation. In addition, small dunes, rills and small obstacle marks with directions at a high angle to the mean channel direction may record rapid flow draining off the higher parts of the bed. Locally, these runoff features may be oriented up-channel recording water flowing off the up-channel side of bars into lows. These may preserve palaeocurrent patterns that are more varied than expected in fluvial systems and may appear similar to some features seen in tidal settings. There is relatively little reworking of pre-existing unit bars.

2. Events in 10 000 to 14 000 $m^3 s^{-1}$ range with gradual decline and large total discharge volume

In events with more gradual decline in discharge, preservation of high stage features is less common. This is because the flow velocity may decline during waning stage such that stationary waves are less frequent and antidunes either do not form or are not preserved because of sediment movement on the bed at later stages of flow. For example, no antidunes are recognized on aerial photographs from some years (for example, 1998, following the event that peaked at 11 905 m^3 s^{-1} with moderately gradual decline). Dunes may be washed out as the water level declines and the bed is mostly characterized by extensive planar sand sheets, gravel sheets and unit bars. Some pre-existing unit bars are likely to be greatly reworked and others washed out.

3. The biggest events (>14 000 m^3 s^{-1})

These events rework large areas of the channel bed and produce new large bedforms and bar forms. Unit bars formed in antecedent events are likely to be removed and new ones formed. GPR data (Fielding *et al*., 1999, 2011) suggest that cross-sets up to 5 m thick are preserved deep in the channel deposits. Vegetation obstacle marks and vegetation-generated bars are likely to be less common in the deposits of these large events because of both the magnitude of the event and the duration of inundation, which will remove a lot of the riverbed vegetation, kill others by the prolonged submergence and bury still more *in situ* by complex bar formation (Fielding *et al*., 1997).

DISCUSSION

The ability of a discharge event to change the morphology of a riverbed and banks is controlled by the rate of **coarse** sediment entrainment and bedload transport, as well as deposition. In this setting, the volume of suspended sediment passing through the channel is of little importance because very little of it is deposited within the channel or on the banks (Alexander & Fielding, 2006). Volume of riverbed sediment reworked and features in deposits may not relate to the peak magnitude of an event. As has been observed in other settings (e.g. Lisle, 1989; Roth *et al*. 2014) the pulses of sediment input and pulses of sediment movement at any one point on the bed may not be in phase with water runoff at that site. This was documented at the Burdekin River study site in March 2000 event (Amos *et al*., 2004) when bedload transport and channel shape change rate were greatest several days after the peak discharge.

Amos *et al*. (2004) estimated that 3 x 10^5 tonnes of bedload were transported past the Inkerman Bridge in the 2000 discharge event that peaked on 25 February at 11 155 m^3 s^{-1}. These authors measured the average bedload transport rate (channel width-integrated) rising rapidly to 0.816 kg s^{-1} m^{-1} on 3 March and then decreasing rapidly to 0.058 kg s^{-1} m^{-1} on 6 March, then more slowly to 0.003 kg s^{-1} m^{-1} on 8 March at the end of the sampling period. If the solid sediment is considered to have a density of quartz (2648 kg m^{-3}) and the deposits in a newly formed unit bar a porosity of 40% then on 3 March 2000 a 1 m high bar slip face could have advanced 1 m in 32.5 minutes, whereas on 6 March 2000 it would have taken 7.6 hours and on 8 March more than six days. The pulses of bedload movement will alter channel morphology by promoting bar migration and as the bedload flux often lags discharge change, most bar modification occurs after peak discharge. This explains why bars are not modified much in short duration large events. This has some similarity to Rushmer's (2007) findings using flume models of jökulhlaup to investigate the control of different hydrograph rising limb shapes on rates of sediment transport, deposition, erosion and bedform development.

Because of the highly variable system, the Burdekin River channel is unlikely to reach a steady-state in any individual discharge event. The amount of work done by a flood depends not only on the peak discharge but also on the duration of exceedance of critical discharges. It takes time to erode bed and banks, such that the channel size and shape may not change much in a short-duration event. There is also the issue of lag time for bed accretion, because not only does it take time to entrain sediment, it also takes time for sediment to move into and down the river. This is particularly well-illustrated by the 2000 event where peak bedload flux lagged peak discharge, and change was supply-limited. Thus, the concept of dominant discharge (defined as that discharge which transports most bed sediment in a stream that is close to steady-state conditions; Carling, 1988) is of little use in settings with very high discharge variability.

Sediment grade is not a good indicator of palaeoflow conditions in these systems. Sediment entrainment and transport is dependent on the bed shear stress, and grade of sediment in deposits is often used as a rough indication of flow depth and velocity. This is complicated in rapidly varying systems such as the Burdekin, because in rapidly changing floods the impulse force due to rapid change must also be considered (Alexander & Cooker, 2016). The velocities recorded in some Burdekin events (e.g. Amos *et al*., 2004) and estimated from antidune morphology (for example, for the 2017 event herein) would produce bed shear stress that could

easily move particles coarser than are commonly seen on the bed. Locally where large clasts are available (for example, road bridge debris) they are moved by big events. For example, a 1 m length of steel guardrail moved about 50 m downstream from a bridge on the Bowen tributary in the 2017 event.

The grade of sediment preserved in a deposit, however, depends not on the transport and entrainment controls but on the depositional conditions, and in a rapidly waning flood these may be significantly different to the peak conditions. The grade also depends on sediment availability and the lag time for coarse sediment to be transported to the site of deposition. At the study site, velocities and bed conditions in big discharge events would be capable of transporting boulder grade particles, but these are rarely available to the site. Grade therefore is a very poor indicator of peak flow conditions even in relatively small events.

Cross-bed set thickness is not a good indicator of palaeoflow conditions in these systems. Cross-bed set thickness has been used as an indicator of flow depth and conditions in interpreting some rock record examples (Leclair & Bridge, 2001), although Bradley & Venditti (2017) argue that there is more variability in the ratio between set thickness and flow depth and more complexity in the controls on dune scale than considered by Leclair & Bridge (2001). The issues of bedform disequilibrium are now well-established (Myrow *et al*., 2018). In the Burdekin River and similar highly variable discharge rivers, dune height and cross-set thickness may be very misleading. This is both because of the speed of change and because of the occurrence of dunes and unit bars together. Because dunes tend to downclimb unit bars, it leads to greater dune-set preservation than would be expected from relationships developed in the laboratory (e.g. Leclair & Bridge, 2001; Reesink *et al*., 2015). Amos *et al.* (2004) pointed out that: *"the lag time for dune formation (particularly bigger forms) is such that there is not a strong correlation between discharge stage and dune size"* in this system where stage can change by several metres in a day or two. As stage rises, dune height and length will tend to increase, but as stage rise is very fast the dune height is likely to continue to rise at and after the peak. In discharge events the very rapid stage rise and fall may prevent dunes ever reaching a size consistent with the magnitude of the peak. In contrast, in the very large floods with longer durations, dunes may grow bigger.

In general, unit bars are larger in volume than dunes, and take longer to change length and height at the same bedload flux. Unit bar height is controlled by the 'profile of equilibrium' (cf. Jopling, 1966), where the sediment transport rate over the top of the unit bar results in a balance

between deposition and erosion of the bar top such that if they are in equilibrium all sediment transported over the bar top is only deposited at the bar lee if it is deposited at all. Some unit bars will be less tall than the superimposed dunes and, in this case, they become very difficult to differentiate and may appear as dune fields. Commonly observed unit bars may have greater amplitude than the associated dunes and they can be much larger. An added complication is that individual unit bars may persist through a number of different magnitude discharge events, whereas dunes may be washed out and reform. Unit bars are ubiquitous and will cause the development of relatively thick down-climbing (i.e. down-current descending) cross-stratified sets, containing numerous smaller cross-bed sets formed by superimposed bedforms (Herbert *et al*., 2019). Locally in larger unit bars, large set thicknesses will develop as lee faces amalgamate.

The very biggest discharge events result in wholesale reworking of complex bars and thus in the preserved deposits it is likely that the lower parts of bar complexes will preserve evidence of bigger bedforms – not as a result of being deeper in the channel but because of their formation in the biggest discharge events. Only near-surface deposits will be reworked somewhat by the smaller magnitude events. This is supported by ground-penetrating radar data that show largest and thickest cross-bed sets and scours at and near the base of sections in both the Inkerman site (Fielding *et al*., 2005b) and at a site upstream near Charters Towers (Fielding *et al*., 1999).

Antidunes and associated sedimentary structures may be a relatively good indicator of depositional conditions. Antidunes formed in sand or fine gravel, unlike dunes, rapidly establish size related to the flow conditions, thus the wavelength of the bedforms, or possibly the size of the resulting lenses (Froude *et al*., 2017) may be a better indicator of flow depth and velocity. The problem with this, however, is that the preserved forms are likely to relate to the falling stage conditions rather than peak flow conditions because they are easily reworked. In addition, they are more likely to be preserved in the deposits from events with rapidly falling stage.

The mean flow velocity can be estimated from the antidune wavelengths using Kennedy's (1961) empirical equation $\lambda = 2\pi V^2/g$, where g is the acceleration due to gravity, V is the mean velocity and λ is antidune wavelength. In 2017, at the Inkerman antidune site (Fig. 1C) when antidunes formed with wavelengths of 16.4 to 28.8 m, velocities at the sites when they formed are estimated as 5.1 to 6.7 m s^{-1}. Given these estimates, using $Fr = V/\sqrt{(gd)}$, where Fr is the Froude Number and d is the flow depth, and assuming that antidunes formed at a Froude Number between 1 and 0.84, it suggests that water depths when they formed were 2.6 to 4.6 m. Wavelength of

antidunes at the Jarvis field site in 2017 were as much as 30.7 m, implying velocity of 6.9 m s^{-1} in 4.9 m depth of flow.

Froude *et al*. (2017) used flume observations by Alexander *et al*. (2001) to develop the idea that in flood deposits, gravel lens length parallel to flow may be used to estimate flow velocity. These authors suggested that mean lens size in one bed may be related to the mean wavelength (temporal and spatial averaging) of the flow that deposited the lenses. If this worked, it would be useful for estimating conditions from deposits when the surface morphology of antidunes is not preserved. Alexander *et al.* (2001) found that, for sand lenses formed from antidunes in a flume, the ratio of mean lens length to measured water-surface wavelength in the flume was between 0.38 and 0.56. Froude *et al*. (2017) applied this with moderate success to estimate flow velocity in a lahar from gravel lenses in its deposit. In the Burdekin River however, at the Inkerman antidune site the gravel lenses formed by the gravel patches at antidune crests appear to be 0.23 to 0.34 of the mean antidune wavelength within antidune trains. If preserved in the deposits, the lenses might be identified by their steep gravel fabric and associated facies, but because of the undersupply of gravel the lens size would underestimate velocities and water depths using Froude *et al*.'s (2017) method unless it becomes possible to estimate the gravel lens to wavelength ratio from the architecture of the deposits. It is postulated here that this might be achieved in an approximate way using the gravel percent in the deposit.

Vegetation obstacle marks and vegetation-generated bars are commonly observed in the Burdekin River and other rivers of this type (Nakayama *et al*., 2002). Preserved *in situ* vegetation and related sedimentary structures recorded in the deposits are considered characteristic of tropical highly variable channel deposits (Fielding *et al*., 2009; 2011). They are observed resulting from all flood types but their abundance and character may vary. This is because scour around obstacles (cf. tree trunks or grass clumps) takes time to develop. It is not true to say that the longer flow conditions are maintained the more scour will develop, as the scour depends on the mobility of the bed sediment and the geometry of the obstacle. That said, the shortest flood events may not reach the maximum depths of scour, such that more vegetation will persist on the bed. Vegetation survival is also influenced by duration of submergence, although it is not known how long submergence of different species in this setting will result in plant mortality.

How did five years of antecedent channel-bed plant growth impact the sedimentary response? Before the arrival of TC Debbie in 2017, the riverbed downstream of Inkerman Bridge

was well covered by tree saplings and other vegetation (Fig. 5A). The runoff in 2017 removed >50% of this vegetation and cut erosional swales through the sapling groves, 2 to 3 m deep and gravel-covered (Fig. 5B). Sediment aggradation occurred around surviving vegetation, producing abundant vegetation obstacle marks and tree-triggered linear bars in a manner previously documented at this site at a smaller scale (Herbert & Alexander, 2018) and at other sites (Fielding *et al*., 1997; Nakayama *et al*., 2002).

CONCLUSIONS

In the lower Burdekin River, over the last 50 years, there have been 23 discharge peaks greater than 10 000 m^3 s^{-1}. These are of three event types. Type 1 events peak between 10 000 and 14 000 m^3 s^{-1}, are short duration and discharge deceases to less than half peak within 24 hours. Type 2 peak in the 10 000 to 14 000 m^3 s^{-1} range with gradual decline (decrease to less than half peak within three days). Type 3 are the biggest events arbitrarily classed >14 000 m^3 s^{-1}; eight of these occurred.

Type 3 events rework large amounts of riverbed and create new bars. Type 2 events rework the bed, change bar position and produce new attached bars but leave areas of Type 3 deposits unchanged (particularly at depth). After both Type 2 and 3 events, bar surfaces are dominantly sand and gravel sheets. Type 1 events rework bar surfaces a little and produce minor bar accretion. After Type 1 events, washed-out dunes dominate bar surfaces and antidunes are preserved. In comparison, antidunes are not observed after Type 2 events where discharge falls more gradually. The differences between Type 1 and Type 2 event deposits highlight that the maximum discharge magnitude does not correlate with the amount of morphological change in the channel. The duration of large discharge events is an important control on the amount of change in morphology and a difference of only a few days can be considerable.

In all of these big events the flow conditions are such that boulders could be entrained, but these are rarely available at the site. Sediment grade in deposits is a very poor indicator of peak flow conditions even in relatively small events.

Due to the co-occurrence of dunes and unit bars, rapid changes in flow depth (such that bedforms do not reach equilibrium with flow conditions) cross-strata set thickness is not a good

indicator of palaeoflow conditions. Cross-strata set thickness is likely to considerably underestimate flow velocity and water depth in these highly variable discharge systems.

Antidunes often form on the riverbed. These are easy to identify where gravel accumulates at the crests but less obvious on sandy areas of the dry bed. Where the bedform dimensions are preserved these are good indicators of velocity and depth at the time of formation. However, in this gravel-poor setting the application of the Froude *et al*. (2017) method for estimating antidune wavelength from gravel lens flow-parallel length is likely to underestimate flow velocity and water depth.

The nature of the sedimentary record, from rivers such as the Burdekin, is a complex mosaic biased towards events of relatively large magnitude that gradually decline to base flow. Unlike in less variable systems, channel deposit size is unlikely to be indicative of a channel-forming discharge. The relative volume of component event deposits may relate more to event duration than to magnitude. If sediments preserve the characteristics of systems with high or very high coefficients of peak discharge variance (as described by Fielding *et al*., 2018), conventional relationships are unlikely to be valid.

ACKNOWLEDGEMENTS

JA and CH thank University of East Anglia for support of fieldwork costs. CRF fieldwork was supported by the Coffman Endowment in Sedimentary Geology at UNL. KA thanks the University of Adelaide Faculty of Engineering, Computer and Mathematical Sciences for providing funding support for research following maternity leave. River discharge data were obtained from the State of Queensland Department of Natural Resources, Mines and Energy (accessed via BOM web site). rainfall and cyclone track data were obtained from BOM available via http://www.bom.gov.au/ (accessed July 2018). Our thanks to Colin North, Ellen Wohl, an anonymous reviewer and Associate Editor Charlie Bristow for constructive criticism that led us to improve this paper.

DATA AVAILABILITY STATEMENT

The rainfall data that support the findings of this study are openly available in the Australian Government Bureau of Meteorology data repository at http://www.bom.gov.au/qld/. The

discharge data that support the findings of this study are openly available in the Australian Government Bureau of Meteorology water data repository at http://www.bom.gov.au/waterdata/. Other data used in this paper is available on request from the authors.

REFERENCES

Ager, D.V. (1973) *The Nature of the Stratigraphic Record*, Wiley, Chichester, 114pp.

Alexander, J. and **Cooker, M**. (2016) Moving boulders in flash floods and estimating flow conditions using boulders in ancient deposits. *Sedimentology*, **63**, 1582-1595.

Alexander, J. and **Fielding, C.R**. (1997) Gravel antidunes in the tropical Burdekin River, Queensland, Australia. *Sedimentology*, **44**, 327-337.

Alexander, J. and **Fielding, C.R**. **(**2006) Coarse-grained floodplain deposits in the seasonal tropics: towards a better facies model, *Journal of Sedimentary Research,* **76**, 539 – 556.

Alexander, J., **Fielding, C.R**. and **Pocock, G.D**. (1999) Flood behaviour of the Burdekin River, Tropical North Queensland, Australia*. In:* Alexander, J. and Marriott, S. (editors) *Floodplains: interdisciplinary approaches,* Geological Society of London Special Publication*,* **163**, 27-40.

Amos, K.J., **Alexander, J**., **Horn, A**., **Pocock, G.D**. and **Fielding, C.R**. (2004) Supply limited sediment transport in a high-discharge event of the tropical Burdekin River, North Queensland, Australia. *Sedimentology,* **51**, 145-162.

Bailey, R.J. and **Smith, D.G**. (2010) Scaling in stratigraphic data series: Implications for practical stratigraphy. *First Break,* 28, 57-66.

Bainbridge, Z.T., **Wolanski, E.**, **Álvarez-Romero, J.G**., **Lewis, S.E**. and **Brodie, J.E**. (2012) Fine sediment and nutrient dynamics related to particle size and floc formation in a Burdekin River flood plume, Australia*. Marine Pollution Bull*. **65**, 236-248.

Bainbridge, Z.T., **Lewis, S.E**., **Smithers, S.G**., **Kuhnert, P.M**., **Henderson, B.L**. and **Brodie, J.E.** (2014) Fine-suspended sediment and water budgets for a large, seasonally dry tropical catchment: Burdekin River catchment, Queensland, Australia. *Water Resources Research*, 9067-9087. 10.1002/2013WR014386.

Bainbridge, Z., **Lewis, S**., **Smithers, S**., **Wilkinson, S**., **Douglas, G**., **Hillier, S**. and **Brodie, J**. (2016) Clay mineral source tracing and characterisation of Burdekin River (NE Australia) and flood plume fine sediment. *Journal of Soils & Sediment*, **16**, 687-706.

Bainbridge, Z., **Lewis, S**., **Bartley, R**., **Fabricius**, **K., Collier, C**., **Waterhouse, J., Garzon-Garcia, A., Robson, B., Burton, J., Wenger, A**. and **J. Brodie.** (2018) Fine sediment and

particulate organic matter: A review and case study on ridge-to-reef transport, transformations, fates, and impacts on marine ecosystems. *Marine Pollution Bulletin*, **135**, 1205-1220.

Barclay, J., Alexander, J. and **Sušnik, J**. (2007) Rainfall induced lahars on Montserrat. *Journal of the Geological Society of London*, **164**, 815-227.

Bradley, R.W. and **Venditti, J.G**. (2017) Re-evaluating dune scaling relations. *Earth Science Reviews*, **165**, 356-376.

Bridge, J.S., Alexander, J, Collier, R.E.Ll., Gawthorpe, R.L. and **Jarvis, J**. (1995) Ground-penetrating radar and coring used to study the large-scale structure of point-bar deposits in 3 dimensions. *Sedimentology*, **42**, 839-852.

Bridge, J.S., Collier, R., Ll. and **Alexander, J.** (1998) Large-scale structure of Calamus River deposits (braid bars, point bars, and channel fills) revealed using ground-penetrating radar. *Sedimentology*, **45,** 977-986.

Carling, P. (1988) The concept of dominant discharge applied to two gravel-bed streams in relation to channel stability thresholds. *Earth Surface Processes and Landforms,* **13**, 355-367.

Cenderelli, D.A. and **Wohl, E.E**. (2003) Flow hydraulics and geomorphic effects of glacial-lake outburst floods in the Mount Everest region, Nepal. *Earth Surface Processes and Landforms,* **28**, 385-407.

Dott, R.H., Jr. (1983) Episodic sedimentation – how normal is average? How rare is rare? Does it matter? *Journal of Sedimentary Petrology*, **53**, 5-23.

Dzulynski, S. and **Walton, E.K**. (1965) *Sedimentary Features of Flysch and Graywackes*. Elsevier, Amsterdam, 274 pp.

Fielding, C.R., Alexander, J. and **Newman-Sutherland, E**. (1997) Preservation of *in situ* vegetation in fluvial channel deposits - data from the modern Burdekin River of North Queensland, Australia. *Palaeogeography, Palaeoclimatology, Palaeoecology,* **135**, 123-144.

Fielding, C.R., Alexander, J. and **McDonald, R**. (1999) Sedimentary facies from GPR surveys of the modern, upper Burdekin River of north Queensland, Australia: consequences of extreme discharge fluctuations. *In*: Smith, N.D. and Rogers, J. (editors), *Current Research in Fluvial Sedimentology*, International Association of Sedimentologists Special Publication 28, 347-362.

Fielding, C.R., Trueman, J.D. and **Alexander J**. (2005a) Sharp-based, flood-dominated mouth bar sands from the Burdekin River Delta of northeastern Australia: extending the spectrum of mouth bar facies, geometry and stacking patterns. *Journal of Sedimentary Research*, **75**, 55-66.

Fielding, C.R., Trueman, J.D. and **Alexander, J**. (2005b) Sedimentology of the Modern and Holocene Burdekin River Delta of North Queensland, Australia – controlled by river output, not by waves and tides. *In:* Giosan, L. and Bhattacharya, J. (editors), *Deltas, New and Old*: SEPM Special publication 83, 467-496.

Fielding, C.R., Allen, J.P., Alexander J. and **Gibling, M.R.** (2009) Facies model for fluvial systems in the seasonal tropics and subtropics. *Geology*, 37, 623-626.

Fielding, C.R., Allen, J.P., Alexander, J., Gibling, M.R., Rygel, M.C. and **Calder, J.H**. (2011) Fluvial systems and their deposits in hot, seasonal semiarid and subhumid settings: modern and ancient examples, *In:* Davidson, S.K., Leleu, S., and North, C.P. (editors) *From River to Rock Record: The preservation of fluvial sediments and their subsequent interpretation*. SEPM Special Publication 97, 89-111.

Fielding, C. R., Alexander, J. and **Allen, J. P**. (2018) The role of discharge variability in the formation and preservation of alluvial sediment bodies. *Sedimentary Geology,* **365**, 1-20.

Froude, M.J., Alexander, J., Barclay, J and **Cole, P**. (2017) Interpreting flash flood palaeoflow parameters from antidunes and gravel lenses: An example from Montserrat, West Indies. *Sedimentology*, **64**, 1817–1845.

Graf, W.L. (1983) Downstream Changes in Stream Power in the Henry Mountains, Utah. *Annals of the Association of American Geographers,* **73**, 373-387.

Groisman, P.Ya., Knight, R.W., Easterling, D.R., Karl, T.R., Hegerl, G.C. and **Razuvaev, V.N.** (2005) Trends in intense precipitation in the climate record. *Journal of Climate,* **18**, 1326-1350.

Hajek, E.A. and **Straub, K.M**. (2017). Autogenic Sedimentation in Clastic Stratigraphy. *Annual Review of Earth and Planetary Sciences,* **45**, 681-709.

Harvey, A.M. (1984) Geomorphological response to an extreme flood: A case from southeast Spain. *Earth Surface Processes and Landforms,* **9**, 267-279.

Herbert, C.M., and **Alexander, J**. (2018) Bottomset architecture formed in the troughs of dunes and unit bars. *Journal of Sedimentary Research*, **88**, 1–32.

Herbert, C., Alexander, J., Amos, K.J. and **Fielding C.R**. (2020) Unit bar architecture in a highly-variable fluvial discharge regime: examples from the Burdekin River, Australia. *Sedimentology*, **67**, 576-605.

Horn, J.D., Fielding, C.R., and **Joeckel, R.M**. (2012) Revision of Platte River alluvial facies model through observations of extant channels and barforms, and subsurface alluvial valley fills. *Journal of Sedimentary Research*, **82**, 72-91.

Joeckel, R.M., and **Henebry, G.M**. (2008) Channel and island change in the lower Platte River, Eastern Nebraska, USA: 1855-2005. *Geomorphology*, **102**, 407-418.

Kuhnert, P. M., Henderson, B. L., Lewis, S. E., Bainbridge, Z. T., Wilkinson, S. N. and **Brodie, J. E**. (2012) Quantifying total suspended sediment export from the Burdekin River catchment using the loads regression estimator tool. *Water Resources Research,* **48**, W04533, doi:10.1029/2011WR011080.

Lewis, S.E., Bainbridge, Z.T, Kuhnert, P.M., Sherman, B.S., Henderson, B., Dougall, C., Cooper, M. and **J.E. Brodie.** (2013) Calculating sediment trapping efficiencies for reservoirs in tropical settings: A case study from the Burdekin Falls Dam, NE Australia. *Water Resources Research*, **49**, 1017–1029, doi:10.1002/wrcr.20117.

Lewis, S., Bainbridge, Z. Stevens, T. Garzon-Garcia, A. Chen, C. Burton, J. Bahadori, M. Rezaei Rashti, M. Gorman, J. Smithers, S. Olley, J. Moody, P. and **Dehayr, R.** (2018) Sediment tracing from the catchment to reef 2016 to 2018: Flood plume, marine sediment trap and logger data time series. Report to the National Environmental Science Program. Reef and Rainforest Research Centre Limited, Cairns 94pp.

Lisle, T.E. (1989) Sediment transport and resulting deposition in spawning gravels, north costal California. *Water Resources Research,* **25**, 1303-1319.

Maher, B.A., Watkins, S.J., Fielding, C.R., Alexander, J. and **Brunskill, G.** (2009) Sediment sourcing by magnetic 'fingerprinting' of transportable sand fractions in a tropical fluvial, estuarine and marine context. *Sedimentology*, **56**, 841-861.

McCulloch, M., Fallon, S., Wyndham, T., Hendy, E., Lough. J and **Barnes, D**. (2003) Coral record of increased sediment flux to the inner Great Barrier Reef since European settlement. *Nature*, **421**, 727–730.

Mitchell, A.W. and **Furnas, M. J**. (1996) Terrestrial inputs of nutrients and suspended sediments to the GBR lagoon. In: *The Great Barrier Reef: Science, Use and Management*: A National Conference, Proceedings, vol. 1, pp. 59–71., November 1996, James Cook Univ., Townsville.

Myrow, P.M., Jerolmack, D.J. and **Taylor Perron, J. (**2018) Bedform disequilibrium. *Journal of Sedimentary Research*, **88**, 1096-1193.

Nakayama, K., Fielding, C.R. and **Alexander, J.** (2002) Variation in character and preservation potential of vegetation-induced obstacle marks in the variable discharge Burdekin River of north Queensland, Australia. *Sedimentary Geology*, **149**, 199-218.

Nanson, G.C. (1986) Episodes of vertical accretion and catastrophic stripping: a model of disequilibrium flood-plain development. *Geological Society of America Bulletin* **97**, 1467-1475.

Neil, D.T., Orpin, A.R., Ridd, P.V. and **Yu, B.** (2002) Sediment yield and impacts from river catchments to the Great Barrier Reef lagoon. *Australian Journal of Marine and Freshwater Research,* **53**, 733-752.

Paola, C., Ganti, V., Mohrig, D., Runkel, A.C. and **Straub, K.M**. (2018) Time Not Our Time: Physical Controls on the Preservation and Measurement of Geologic Time. *Annual Review of Earth and Planetary Sciences,* **46**, 409-438.

Prosser, I.P., Moran, C.J., Lu, H., Scott, A., Rustomji, P., Stevenson, J., Priestly, G., Roth, C.H. and **Post, D.** (2002) Regional patterns of erosion and sediment transport in the Burdekin River catchment. CSIRO Land and Water, Technical Report 5/02, 44.

Reesink, A.J.H., Van den Berg, J.H., Parsons, D.R., Amsler, M.L., Best, J.L., Hardy, R.J., Orfeo, O. and **Szupiany, R.N**., 2015. Extremes in dune preservation: Controls on the completeness of fluvial deposits. *Earth-Science Reviews*, **150**, 652-665.

Rose, C.W., Shellberg, J.G. and **Brooks, A.P**. (2015) Modelling suspended sediment concentration and load in a transport-limited alluvial gully in northern Queensland, Australia. *Earth Surface Processes and Landforms*, **40**, 1291-1303.

Roth, D.L., Finnegan, N.J., Brodsky, E.E., Cook, K.L., Stark, C.P. and **Wang, H.W**. (2014) Migration of a coarse fluvial sediment pulse detected by hysteresis in bedload generated seismic waves. *Earth and Planetary Science Letters*, **404**, 144-153.

Rushmer, E.L. (2007) Physical-scale modelling of jökulhlaups (glacial outburst floods) with contrasting hydrograph shapes. *Earth Surface Processes and Landforms*, **32**, 954-963.

Rustomji, P., Bennett, N. and **Chiew, F**. (2009) Flood variability east of Australia's Great Dividing Range. *Journal of Hydrology*, **374**, 196-208.

Sadler, P.M. (1983) Is the present long enough to measure the past? *Nature*, **302**, p.752.

Sambrook Smith, G.H., Best, J.L., Ashworth, P.J., Lane, S.N., Parker, N.O., Lunt, I.A., Thomas, R.E. and **Simpson, C.J**. (2010) Can we distinguish flood frequency and magnitude in the sedimentological record of rivers? *Geology*, **38**, 579-582.

Smith, N.D. (1974) Sedimentology and bar formation in the upper Kicking Horse River: a braided outwash stream. *Journal of Geology*, **82**, 205-223.

Tooth, S. (2000) Process, form and change in dryland rivers: A review of recent research. *Earth Science Reviews*, **51**, 67-107.

Williams, G.P. (1978) Bank-full discharge of rivers. *Water Resources Research*, **14**, 1141-1154.

Xiao, Y., Wang, X.H., Ritchie, E.A., Rizwi, F. and **Qiao, L**. (2019) The development and evolution of the Burdekin River estuary freshwater plume during Cyclone Debbie (2017). *Estuarine, Coastal and Shelf Science*, **224**, 187-196.

FIGURES

Figure 1. (**A**) Catchment map showing the location of the study site. Gauging stations are: S, Sellhiem; C, Clare; U, Urannah. Rain gauges: K, Kalamia Estate; M, Majors Creek; AB represents Airlie Beach. (**B**) Location map of area of Clare to coast. (**C**) Satellite image of the study reach during the 2017 dry season (image dated 19/08/2017, obtained from: Google Earth, 2019 CNES/Airbus). The area beyond the channel margins has been faded. Black lines labelled 'A', 'B' and 'C' show the positions of elevation transects presented in Fig. 4. Ellipses labelled 'I' and 'J' identify the antidune sites referred to in the text as Inkerman and Jarvisfield.

Figure 2. (**A**) Time series of discharge recorded at Clare 1978 to 2017, showing the magnitude of peak events and the variation within and between years. The discharge in the Burdekin River has been monitored continuously since 1949 at Clare (52 km from the river mouth; drainage basin above Clare is 129 876 km^2). Burdekin Falls Dam, 108 km upstream of Clare was completed in 1987. (**B**) Hydrographs for 1997 discharge at Sellheim and Clare gauging stations. Data from the State of Queensland Department of Natural Resources, Mines and Energy.

Figure 3. Catchment maps: (**A**) Illustrating the main sub-catchments and the mean rainfall pattern (data from www.bom.gov.au/climate/data/); (**B**) land use after State of Queensland 2018 land use map; (**C**) Simplified geological map based on Prosser *et al*. (2002). (**D**) The tracks of the eye of tropical cyclones that were associated with large rainfall events. The numbers on the tracks are cyclone intensity and 'L' indicates that the tropical cyclone (TC) was downgraded to a 'low'. The rainfall covers a large area around the line of the track. Data from Bureau of Meteorology, bom.gov.au/cyclone/history/.

Figure 4. Elevation data for the 2017 study site at channel cross-sections A, B and C; the locations of these are shown in Fig. 1C. Complete cross-sections obtained from LiDAR data, collected in the 2009 dry season (between 10 June and 10 September; Queensland Government Department of Natural Resources, Mines and Energy): 1m grid size, vertical accuracy ±10 cm (1 σ), horizontal

accuracy ±20 cm (1 σ). Real Time Kinematic GPS survey data (horizontal accuracy ±1 cm, vertical accuracy ±2 cm) were collected from 25 to 28 July 2017.

Figure 5. Photographs taken looking downstream from Inkerman Bridge before and after the 2017 event. (**A**) Photograph taken on 15 July 2016. (**B**) Photograph taken on 22 July 2017. Note the remains of old bridge supports visible in both pictures. The river is approximately 1000 m wide in this view.

Figure 6. Burdekin catchment maps of rainfall for seven days: (**A)** rainfall before the peak of a big discharge event; and (**B**) rainfall after the peak discharge of events discussed in this paper. The seven-day rainfall maps are based on those generated at http://www.bom.gov.au/jsp/awap/rain/archive.jsp.

Figure 7. Hydrographs for some of the events discussed in this paper. **(A**) Hydrographs for the 30 days starting from the peak of the discharge recorded at Clare. The distinction between Type 1 and Type 2 discharge events is seen in the rate of decline of the flood and the flood duration. The 1988 (black line) and 2017 (orange line) events are Type 1, and the others are Type 2. (**B**) The discharge recorded at Clare from 1 January to 1 April 1991, to show the multiple peaks. The discharge data is from the State of Queensland Department of Natural Resources, Mines and available via http://www.bom.gov.au/metadata/catalogue/view/ANZCW0503900339.shtml.

Figure 8. Photographs of facies and features. (**A**) Cobbles lodged in *Melaleuca argentea* sapling *ca* 0.5 m above bed in the 2017 event. The red notebook is 0.20 m long. (**B**) Extensive *sand sheets* occur both as components of unit bars and adjacent to unit bars at all elevations in the channel. This view taken in July 2017 is looking upstream towards the Inkerman bridge. Notice the tyre tracks across the sand from bottom right, giving a sense of scale. (**C**) Mud drape over small dunes in July 2017. The spade is 0.60 m long. (**D**) Where the mud drapes are millimetres thick and resting on coarse sand, desiccation can lead to mud curl formation. In this photograph taken in 2017 the mud was deposited in the lee of a unit bar near the low flow channel. The car tracks indicate the scale. (**E**) Looking down on a gravel sheet in 2017. The spade is 0.60 m long. (**F)** Gravel sheet 2017. The blue line is about 0.5 m long.

Figure 9. Photographs of bedforms and features: (**A**) Antidunes appear as elongate gravel patches. The person in the background is 1.80 m tall. **(B**) Antidunes shown in plan and cross-section. The deposits consist of a lens of sandy gravel. The yellow notebook is 0.20 m long. (**C**) Unit bar, the

spade is 0.60 m long. (**D**) Section through unit bar, the spade is 0.60 m long. (**E**) Vegetation obstacle marks, the rucksack is 0.50 m tall. **(F)** Vegetation-generated bar formed around *in situ* trees. The bar was about 1.5 m high, tens of metres long in a grove of mature *Melaleuca argentea* trees near the low water channel of the Bowen River upstream of the Mt Wyatt crossing. This bar was covered by a surface carapace of pebble to cobble gravel. The cut face in the photograph revealed that much of this bar is made up of medium-grained sand, with minor very fine-grained and fine-grained sand lenses, gravelly sand lens, and minor mud partings. Sand beds are arranged in a complex cross-cutting pattern indicating multi-directional cross-bedding as the dominant internal structure. The red notebook on top of the bar is 0.20 m long

TABLES

Table 1. Weather conditions and peak discharge of flow events with peak magnitude greater than 10 000 m^3 s^{-1} since 1977. The largest class of events' peak discharges are highlighted in bold. Discharge data from the State of Queensland Department of Natural Resources, Mines and Energy. Weather data from Australian Government Bureau of Meteorology.

Table 1. Weather conditions and peak discharge of big flow events in the Burdekin River since 1977 (TC = Tropical Cyclone). Discharge data from Australian Government Bureau of Meteorology.

Year month	**Peak discharge at Clare (m^3 s^{-1})**	**Event type**	**Contributing weather**	**Contributing areas**
1978				
February	15266	3	TC Gwen started in the Gulf of Carpentaria and tracked south-east across Cape York	Rain over the entire catchment, heaviest in the east
1979				
March	12795	2	TC Kerry over the Coral Sea moved up and down along the coast	Intense rainfall particularly in east of the catchment
1981				
January	11527	2	Monsoon development. No TC	Rain over the entire catchment, heaviest in the north and on the eastern fringes
1983				
May	12415	2	Monsoon development. No TC	Heavy rain over the entire catchment, heaviest in centre and east
1988				
March	10029	1	TC Charlie tracked south-west from the Coral Sea, making landfall south-east of Townsville (Fig. 1A). Once making landfall, it travelled *ca* 150 km inland over	Rain mostly in the centre and east of the catchment, heaviest in the east

			the eastern parts of the catchment	
1989				
April	14924	3	TC Aivu made landfall near the mouth of the Burdekin River on 4 April and moved west across the catchment	Heavy rain along east of the catchment, moved west across the catchment
1991				
January	15709	1	Well-developed monsoon, with addition of a tropical low over the Bowen subcatchment in February	Intense rain in east of catchment in early January. Widespread rain in January–February, with added intense rain over Bowen subcatchment in February associated with tropical low
	12632	2		
February	29825	3		
	12269	2		
	20002	3		

1998				
January	11905	2	Low pressure light rain followed by monsoon trough and then three TCs in the Coral Sea (for example, TC Katrina; Fig. 3) produced rain on coast	Rain mostly in the north and centre of the catchment, heaviest in the north
2000				
February	11155	2	TC Steve's centre tracked north of catchment (Fig. 3). This was followed by the monsoon trough moving north up the coast and inland	Rain mostly in north of catchment from TC Steve. Monsoon trough rain was widespread and heavier along the coast
2007				
February	12590	2	Monsoon trough. TC Nelson (Fig. 3) may have caused some of the rainfall after the peak event	Rain over the entire catchment, heaviest in the east and north
2008				
January	10215	2	Ex-TC Helen tracked south in January and then a monsoon trough developed in February	Widespread rain produced triple-peak hydrograph
February	23908	3		
February	15005	3		
2009				
February	19515	3	Active monsoon trough resulted in the development of TC Ellie. TC Ellie made landfall north of Townsville and tracked to Gulf of Carpentaria. A trough then formed over the NW Coral Sea	Widespread rain with intense rain in south of the catchment later producing second peak
February	15969	3		
2010				
December	10585	2	Monsoon trough. No TC	Rain over the entire catchment, heaviest in the north as well as the eastern and southern

				fringes
2011				
February	10 180	2	TC Yasi made landfall north of Townsville and moved inland	Rain over the northern parts of catchment and the delta
2012				
March	17144	3	A tropical low tracked across the catchment from west to east	Widespread rain over the catchment
2017				
March	11955	1	TC Debbie made landfall close to the eastern catchment and tracked inland, south-west and then south (Fig. 3). Intense rain was limited to the south and east	Rain short duration and intense on the east of the catchment, heaviest on the eastern fringes

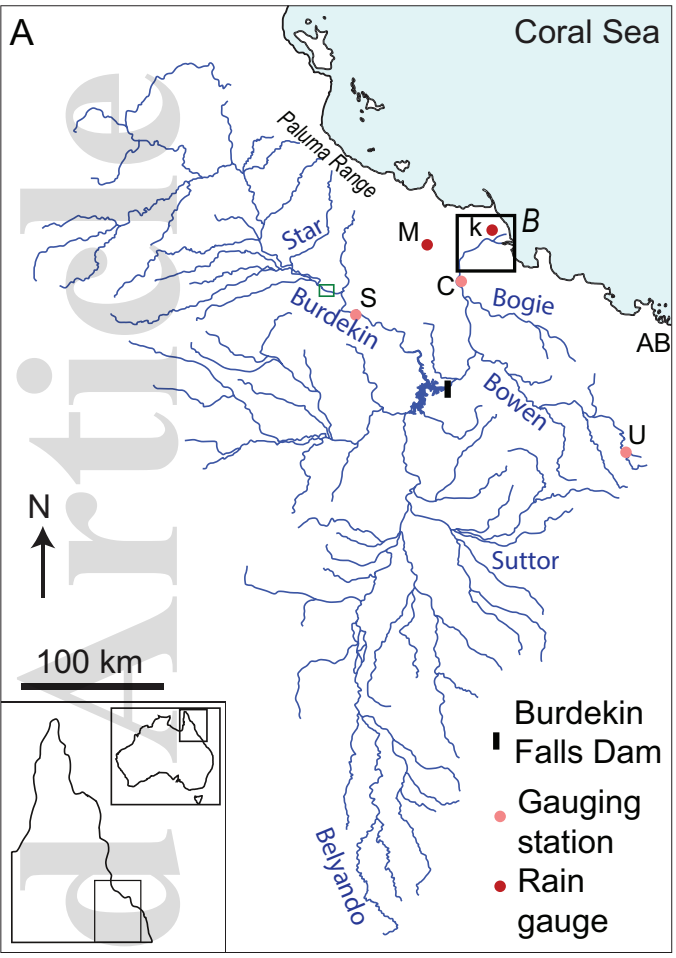

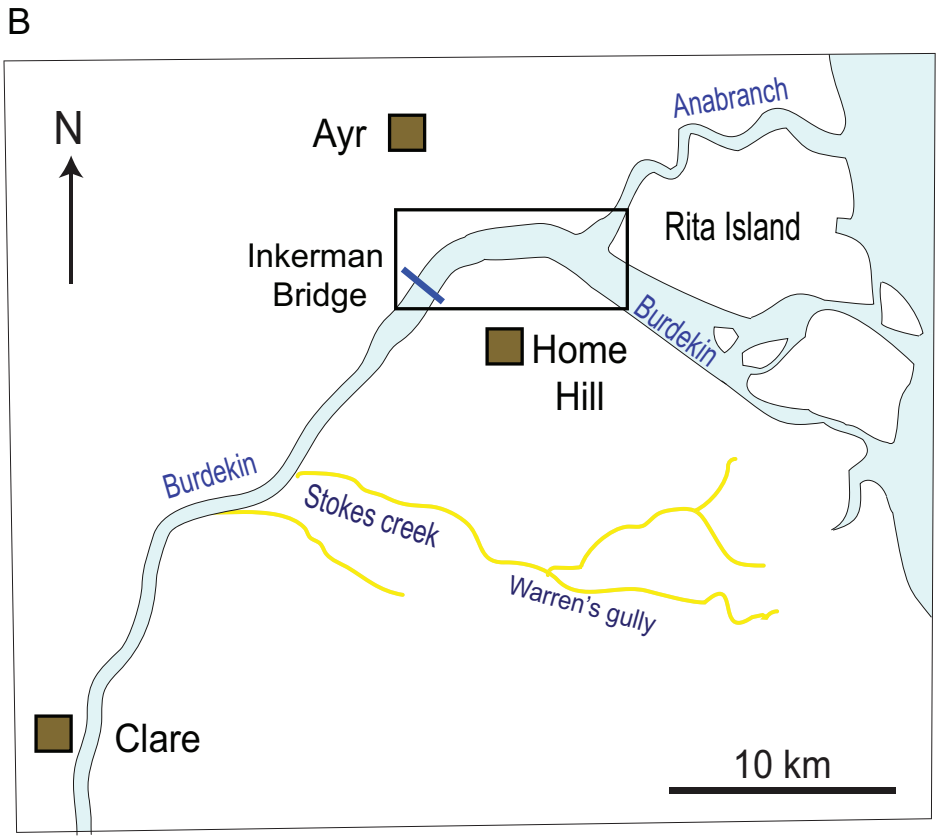

sed_12717_f1.eps

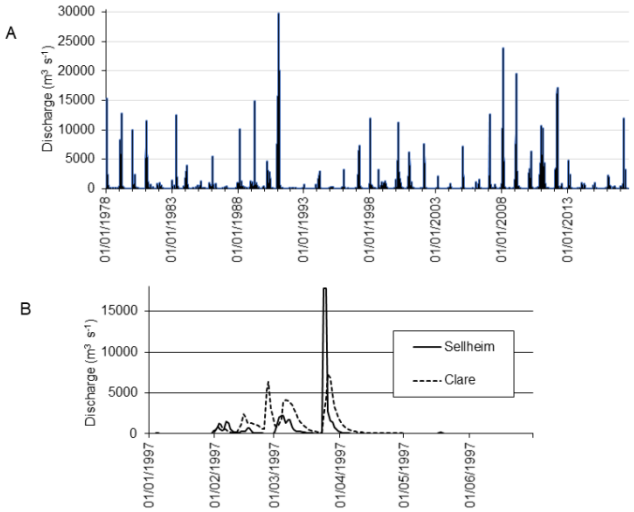

sed_12717_f2.tif

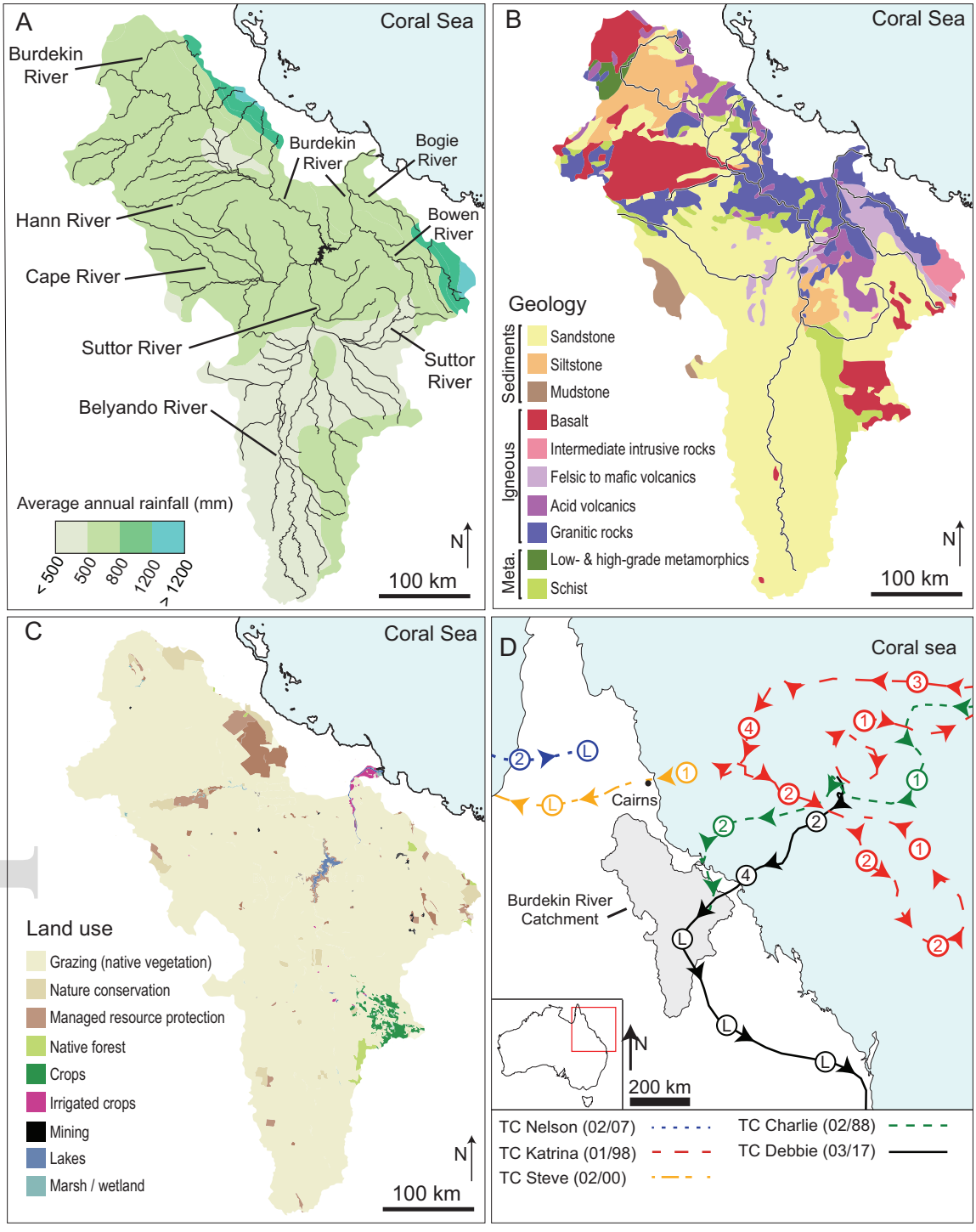

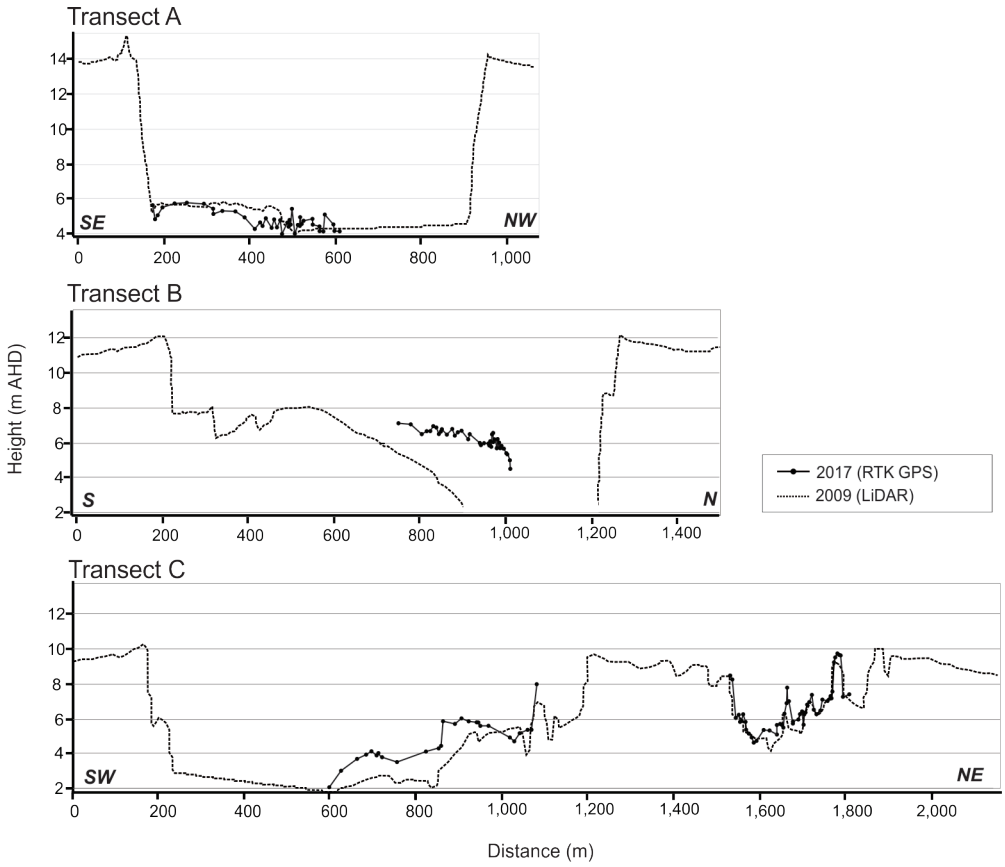

sed_12717_f4.tif

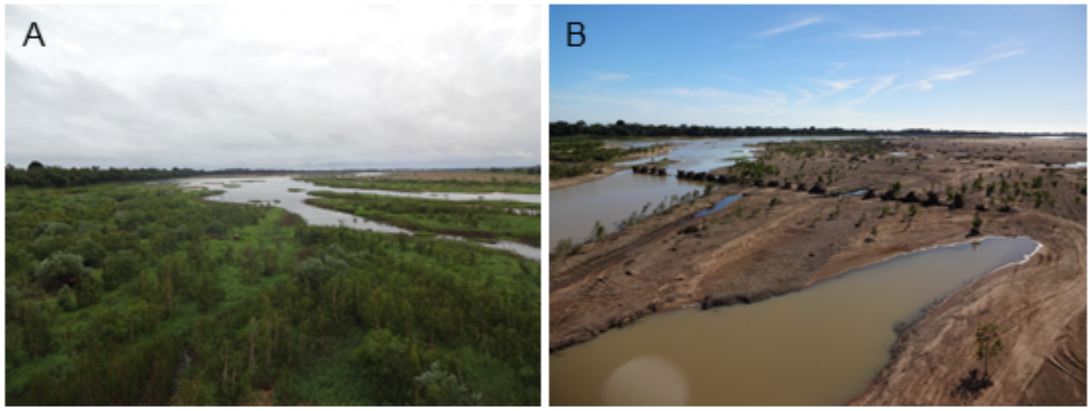

sed_12717_f5.tif

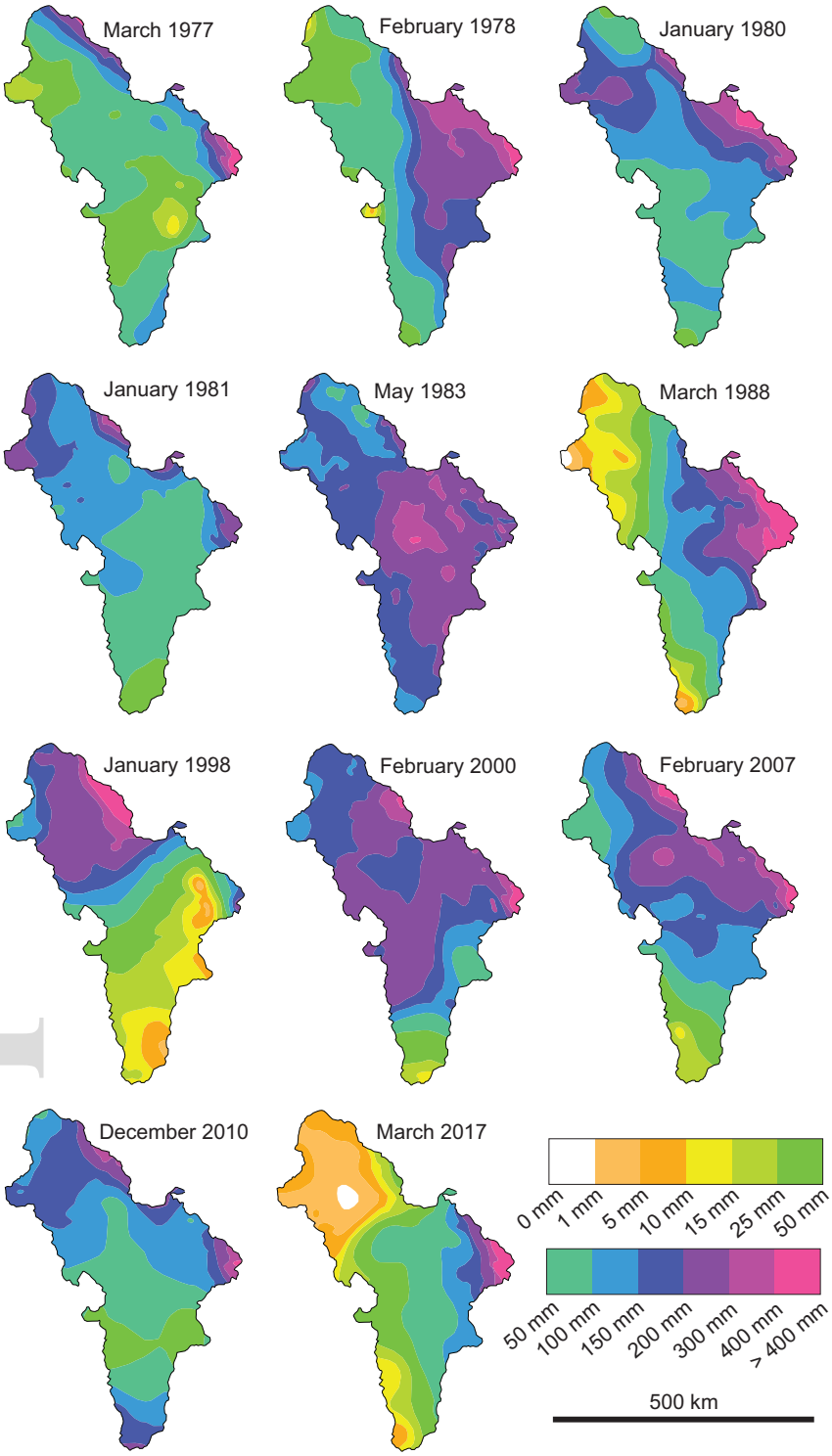

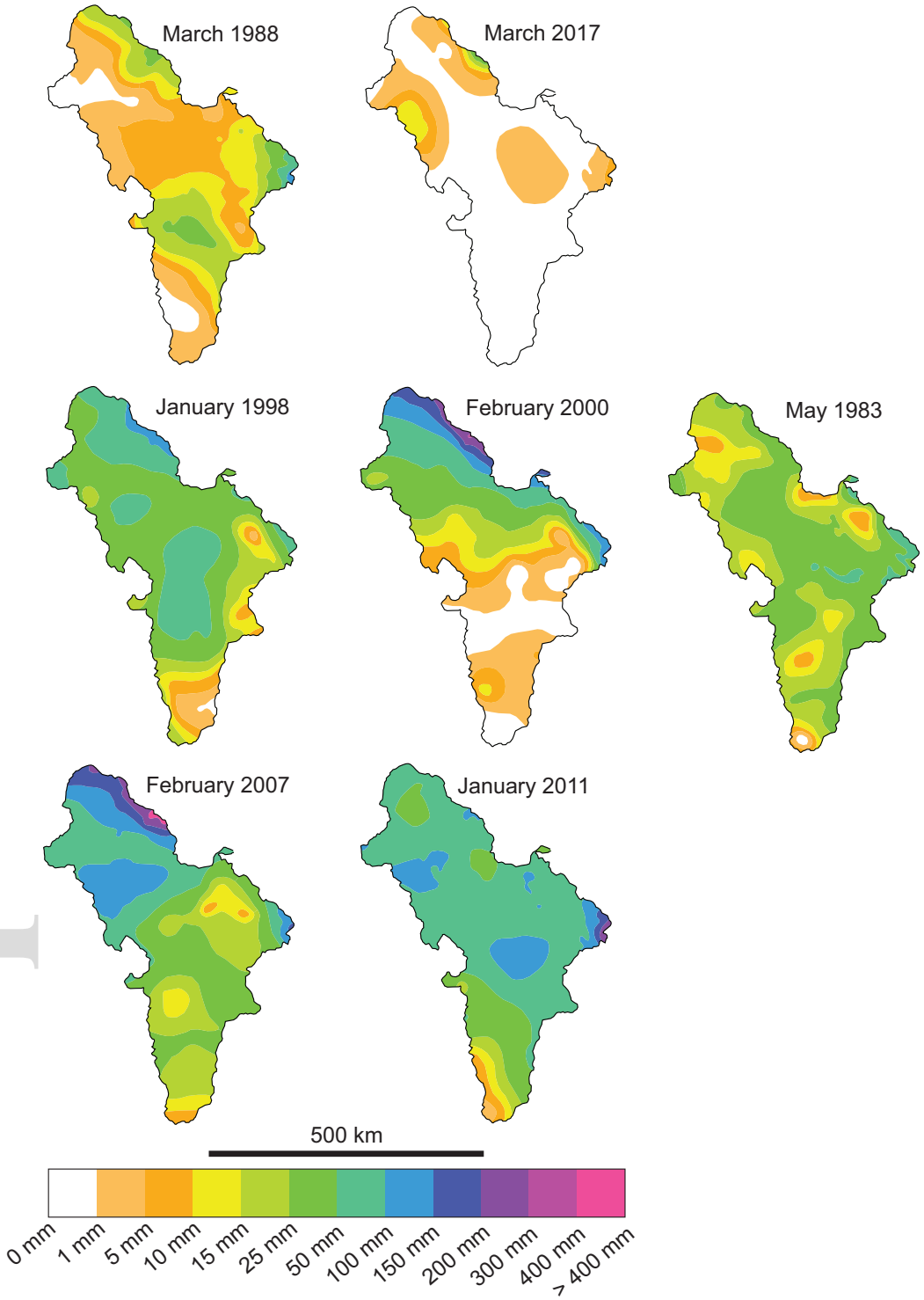

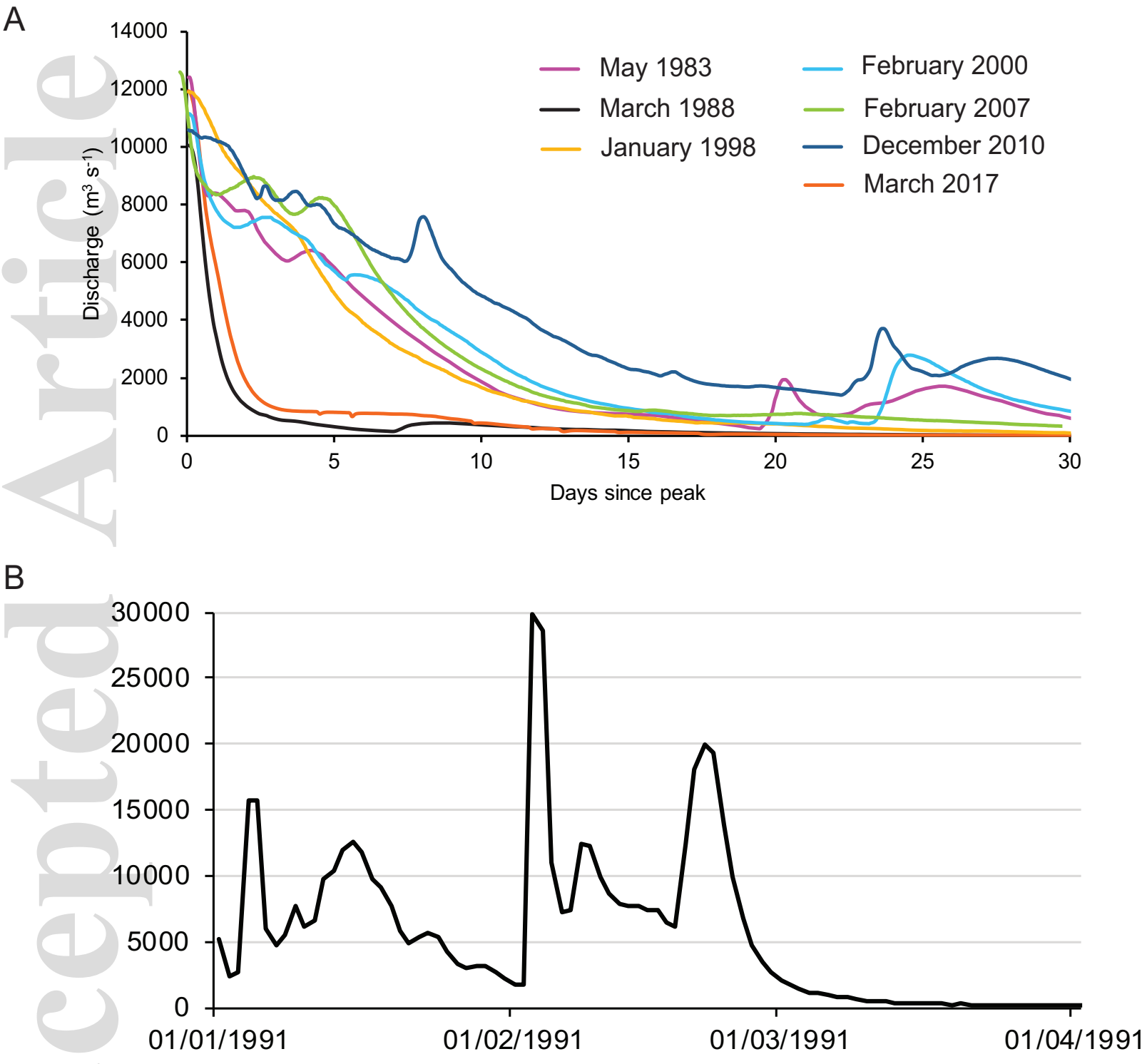

sed_12717_f7.eps

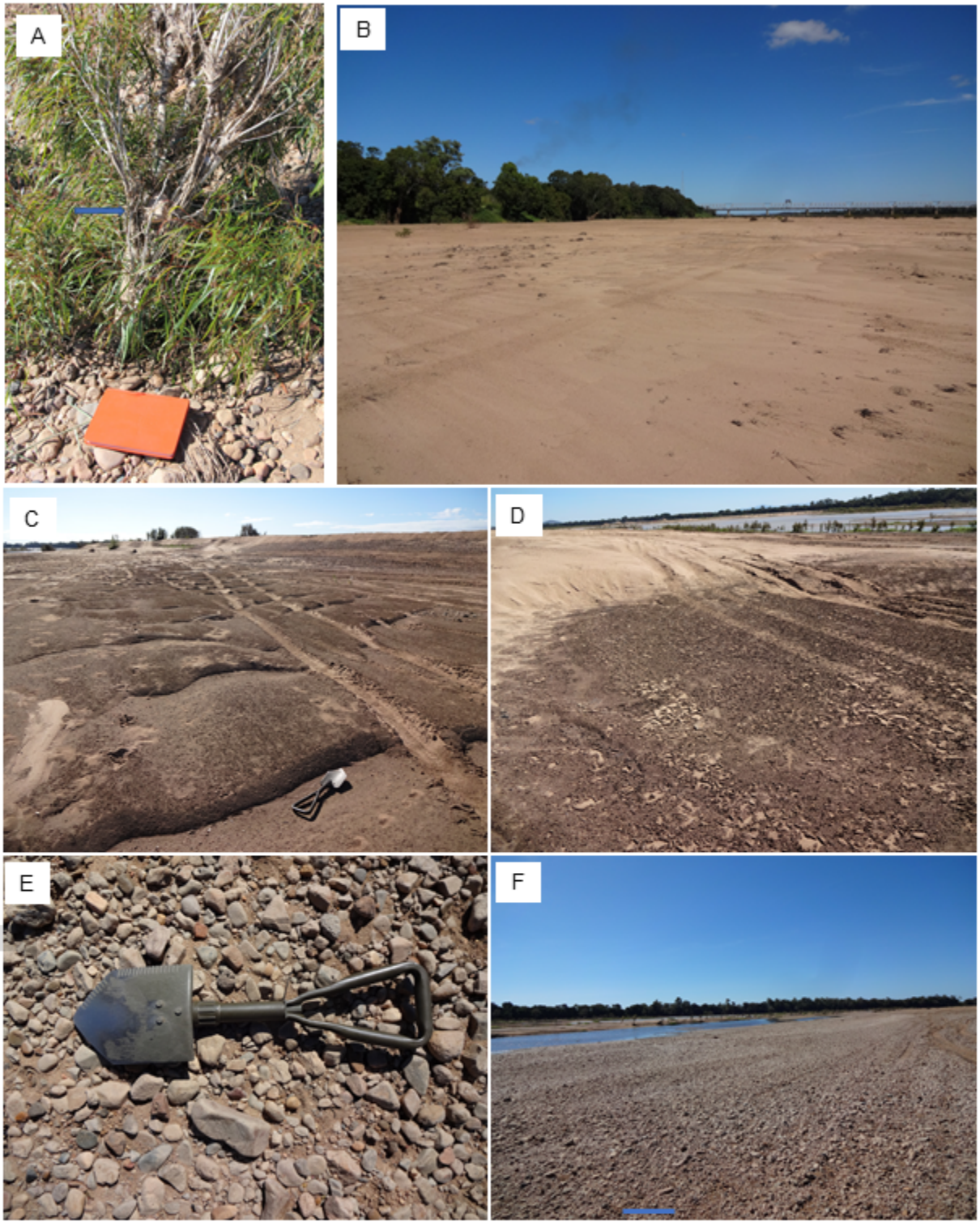

sed_12717_f8.tif

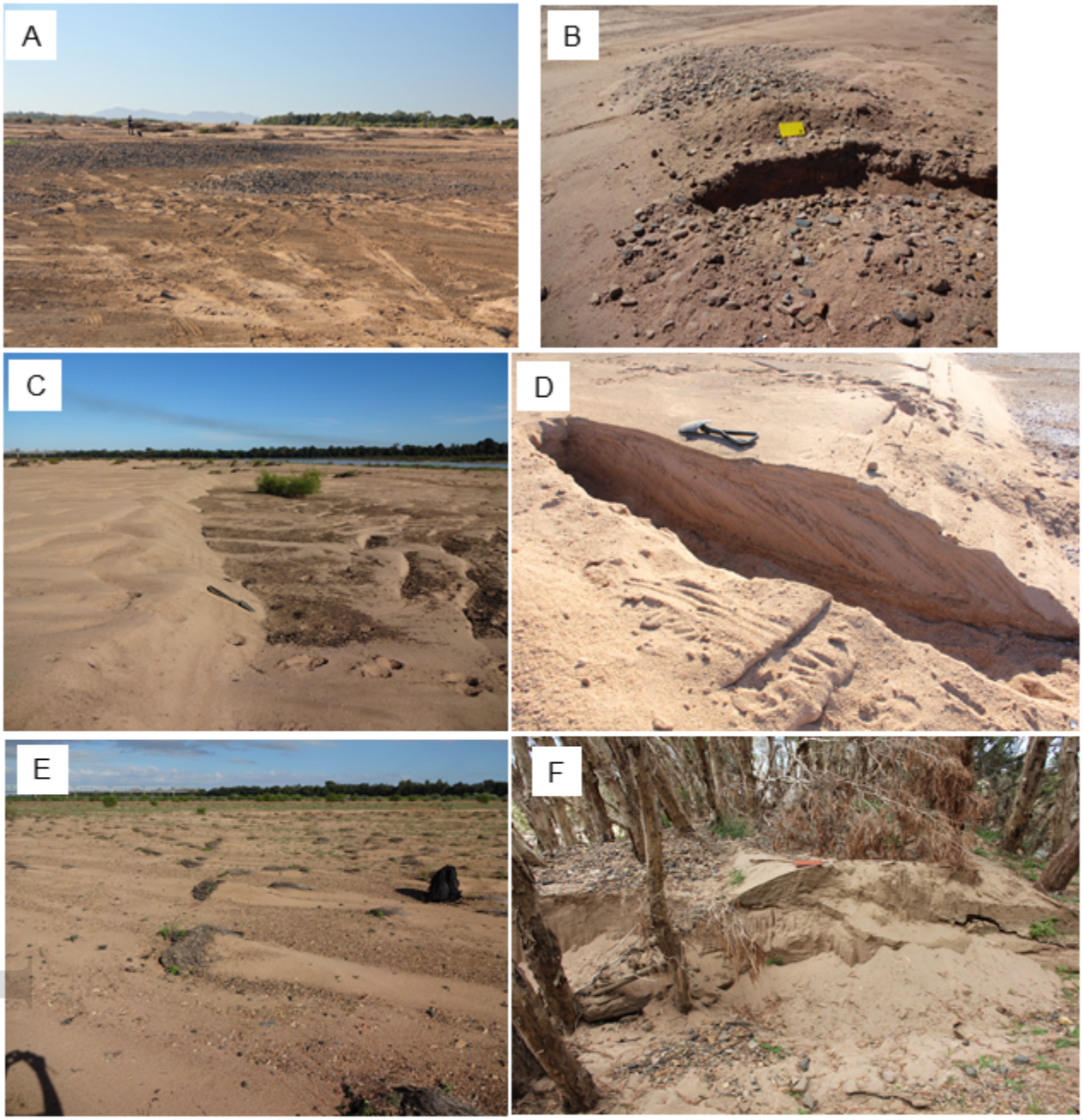

sed_12717_f9.tif